2020

Prospective Isolation And Characterization Of Mononucleated And Binucleated Cardiomyocytes

Rebecca Windmueller
University of Pennsylvania

Prospective Isolation And Characterization Of Mononucleated And Binucleated Cardiomyocytes

Abstract

Loss of cardiomyocytes through cardiac injury and disease substantially impairs cardiac function. Given that cardiomyocytes permanently exit the cell cycle soon after birth, the heart has traditionally been considered a terminally differentiated organ, and thus unable to effectively regenerate. However, recent discoveries have challenged this paradigm and have provided the foundation for exploring the prospect of inducing cardiomyocytes to reenter the cell cycle and, in turn, regenerate damaged myocardium. This has proven challenging, as mammalian cardiomyocytes appear to lose competency to respond robustly to pro-proliferative stimuli following a neonatal maturation period. During this maturation period, cardiomyocytes exit the cell cycle, undergo structural and metabolic changes, and most become binucleated. We and others have observed that the small percentage of mature cardiomyocytes that remain mononucleated (MoNuc) are more competent to respond to proliferative stimuli than their binucleated (BiNuc) counterparts and therefore offer a biological model with which to interrogate loss of proliferative competency in cardiomyocytes. We hypothesized that differences in the maturation processes of MoNucs and BiNucs leave them differentially primed to respond to proliferative stimuli. We devised a novel method to obtain populations highly enriched in MoNuc and BiNuc cardiomyocytes by fluorescence associated cell sorting (FACS) and profiled the transcriptional differences between MoNuc and BiNuc cardiomyocytes at three different timepoints spanning cardiomyocyte maturation. Transcriptome analysis revealed that during the neonatal period, binucleation is associated with the termination of a proliferation-associated gene expression program in exchange for a mature cardiomyocyte gene expression program. Our data also suggested that an E2f/Rb transcriptional network is central to the divergence of these two populations and that remnants of the differences acquired during the neonatal period remain in adult cardiomyocytes. Furthermore, we induced binucleation by genetically blocking the ability of cardiomyocytes to complete cytokinesis, which allowed us to directly link binucleation to changes in Rb/E2f signaling and loss of regenerative competency. The research presented in this dissertation suggests a potential mechanism by which the binucleation process may result in loss of regenerative capacity.

Degree Type

Dissertation

Degree Name

Doctor of Philosophy (PhD)

Graduate Group

Cell & Molecular Biology

First Advisor

Edward E. Morrisey

Keywords

binucleated, cardiac, cardiomyocytes, mononucleated, regeneration

Subject Categories

Biology | Cell Biology | Molecular Biology

PROSPECTIVE ISOLATION AND CHARACTERIZATION OF

MONONUCLEATED AND BINUCLEATED CARDIOMYOCYTES

Rebecca Windmueller

A DISSERTATION

in

Cell and Molecular Biology

Presented to the Faculties of the University of Pennsylvania

in

Partial Fulfillment of the Requirements for the

Degree of Doctor of Philosophy

2020

Supervisor of Dissertation

_____

Edward E. Morrisey, Ph.D., Professor of Medicine

Graduate Group Chairperson

_____

Daniel S. Kessler, Ph.D., Associate Professor of Cell and Developmental Biology
Chair, Cell and Molecular Biology Graduate Group

Dissertation Committee

Zoltan P. Arany, M.D., Ph.D., Professor of Medicine
Christopher J. Lengner, Ph.D., Associate Professor of Biomedical Sciences
Sarah E. Millar, Ph.D., Emeritus Professor of Dermatology
Benjamin L. Prosser, Ph.D., Assistant Professor of Physiology
Ben Z. Stanger, M.D., Ph.D., Hanna Wise Professor in Cancer Research

PROSPECTIVE ISOLATION AND CHARACTERIZATION OF MONONUCLEATED AND BINUCLEATED CARDIOMYOCYTES

Dedicated to the scientists in my family who came before me,

whose guidance, inspiration, and genes have led me here.

Herbert G. Windmueller, PhD
Paternal Grandfather
Scientist emeritus,
National Institutes of Health

Irwin J. Kopin, MD
Maternal Grandfather
Scientist emeritus,
National Institutes of Health

Alan S. Kopin, MD
Uncle
Professor of Medicine,
Tufts Medical Center

ACKNOWLEDGMENT

First, I would like to thank my thesis advisor, Ed Morrisey, for believing in me enough to take me on as a graduate student in his lab and for providing the environment in which I grew into a scientist. I sincerely appreciate the balance he uses in his mentorship that allows his graduate students to pursue their own ideas while still receiving the support needed to ensure success.

I feel incredibly fortunate to have had Drs. Ben Stanger, Ben Prosser, Sarah Millar, Chris Lengner, and Zolt Arany on my thesis committee. They have always been generous with their honest feedback, expertise, support, and encouragement, and that has been greatly appreciated.

I would also like to thank all of the members of the Morrisey Lab, past and present, who have made the lab such a collaborative and supportive environment. I am especially grateful to my "lab siblings" Mindy Snitow, Michael Herriges, Ian Penkala, and Derek Liberti. Mindy and Michael were senior graduate students when I joined the lab and so patiently taught me new techniques and answered my endless questions. Ian and Derek joined the lab during my later years and have been unbelievably supportive and my biggest cheerleaders. On more than one occasion, they also checked plugs or did histology washes for me on weekends when I couldn't come to the lab, and I could not be more grateful to them.

There are several people and groups who have contributed essential parts of the work presented in this dissertation, and I would like to thank them. Mike Morley and Apoorva Babu did all of the bioinformatic analysis of sequencing data. Su Zhou and the CVI histology core sectioned and stained tissue. John Leach performed the neonatal LAD ligation surgeries and provided expertise in the field of cardiac regeneration that I very much appreciate. I am also very grateful to CHOP's Flow Cytometry Core Facility for their support, patience, and willingness to allow me to use their technology in ways they were not used to. During the early part of my dissertation work, I collaborated closely with Ben Prosser's lab, and they were always extremely generous in sharing their cells, protocols, and reagents. The data that resulted from this collaboration directed the path of my dissertation work, so I am especially grateful to them.

Finally, I would like to express my gratitude to the Cell and Molecular Biology Graduate group and the Developmental, Stem Cell, and Regenerative Biology program. Thank you to Dan Kessler, Steve DiNardo, Mary Mullins, Meagan Schofer, and Christina Strathearn. Steve was especially supportive during challenging times that arose during my graduate school training, and I will always be appreciative of that.

ABSTRACT

PROSPECTIVE ISOLATION AND CHARACTERIZATION OF MONONUCLEATED AND BINUCLEATED CARDIOMYOCYTES

Rebecca Windmueller

Edward E. Morrisey

Loss of cardiomyocytes through cardiac injury and disease substantially impairs cardiac function. Given that cardiomyocytes permanently exit the cell cycle soon after birth, the heart has traditionally been considered a terminally differentiated organ, and thus unable to effectively regenerate. However, recent discoveries have challenged this paradigm and have provided the foundation for exploring the prospect of inducing cardiomyocytes to reenter the cell cycle and, in turn, regenerate damaged myocardium. This has proven challenging, as mammalian cardiomyocytes appear to lose competency to respond robustly to pro-proliferative stimuli following a neonatal maturation period. During this maturation period, cardiomyocytes exit the cell cycle, undergo structural and metabolic changes, and most become binucleated. We and others have observed that the small percentage of mature cardiomyocytes that remain mononucleated (MoNuc) are more competent to respond to proliferative stimuli than their binucleated (BiNuc) counterparts and therefore offer a biological model with which to interrogate loss of proliferative competency in cardiomyocytes. We hypothesized that differences in the maturation processes of MoNucs and BiNucs leave them differentially primed to respond to

proliferative stimuli. We devised a novel method to obtain populations highly enriched in MoNuc and BiNuc cardiomyocytes by fluorescence associated cell sorting (FACS) and profiled the transcriptional differences between MoNuc and BiNuc cardiomyocytes at three different timepoints spanning cardiomyocyte maturation. Transcriptome analysis revealed that during the neonatal period, binucleation is associated with the termination of a proliferation-associated gene expression program in exchange for a mature cardiomyocyte gene expression program. Our data also suggested that an E2f/Rb transcriptional network is central to the divergence of these two populations and that remnants of the differences acquired during the neonatal period remain in adult cardiomyocytes. Furthermore, we induced binucleation by genetically blocking the ability of cardiomyocytes to complete cytokinesis, which allowed us to directly link binucleation to changes in Rb/E2f signaling and loss of regenerative competency. The research presented in this dissertation suggests a potential mechanism by which the binucleation process may result in loss of regenerative capacity.

TABLE OF CONTENTS

LIST OF TABLES

LIST OF FIGURES

CHAPTER 1: BACKGROUND AND APPROACH

1.1 INTRODUCTION

Acute myocardial infarction can result in the loss of upwards of one billion cardiomyocytes (Murry et al., 2006). The adult mammalian heart is unable to effectively replace these lost cardiac muscle cells, and instead, undergoes a maladaptive remodeling process that includes hypertrophy and fibrotic scar formation. These events severely impair the ability of the heart to generate force and can often progress to heart failure (Braunwald and Bonow, 2012). Given its response to injury, the heart has traditionally been considered a terminally differentiated organ, incapable of regeneration (Porrello and Olson, 2014). However, as our understanding of cardiac biology has grown more complex, this dogma has been increasingly challenged. The result has been the emergence of the field of cardiac regeneration—the search for a means to replace cardiomyocytes lost through injury.

1.2 APPROACHES TO CARDIAC REGENERATION

Several different schools of thought have materialized on how cardiac regeneration may be facilitated. The research approaches taken can be generally categorized by the potential source of replacement cardiomyocytes they investigate.

Endogenous stem cells

Considerable effort has gone into determining whether a population of stem or progenitor cells exists in the heart, analogous to the population of satellite cells responsible for regenerating skeletal muscle (Beauchamp et al., 1999; Mauro, 1961). Initial reports suggested a stem cell population, which could be identified by cell surface expression of receptor tyrosine kinase c-kit, exists in the adult mammalian heart and is capable of differentiating into new cardiomyocytes (Beltrami et al., 2003). While this area of research has been clouded by controversy, a consensus now holds that these cells do not represent a potential source for cardiomyocyte renewal (Eschenhagen et al., 2017; Ozkan, 2019).

Exogenous stem cells

Another active area of research focuses on transplanting exogenously sourced cardiac myocytes that have been differentiated from embryonic stem cells (ES cells) or induced pluripotent stem cells (iPS cells) (Kehat et al., 2001; Mauritz et al., 2008). While this approach is compelling, several significant roadblocks have come to light. Despite efforts to optimize differentiation and maturation strategies, a significant challenge remains that ES- and iPS-derived myocytes do not fully recapitulate mature myocytes. Stem cell-derived cardiomyocytes resemble immature embryonic cardiomyocytes both structurally and functionally and have reduced capacity for force generation, excitation-

contraction coupling, and energy production (Yang et al., 2014). However, it is not clear whether the maturation state of transplanted cells affects their ability to integrate into a recipient heart successfully. Upon transplantation into non-human primates, ES-derived myocytes do appear to partially integrate into the myocardium but caused arrhythmias in all treated animals (Chong et al., 2014). Therefore, the potential held by these cells to contribute to cardiac regeneration remains to be determined.

Reprogramming of mature cells

The discovery that differentiated cells, such as fibroblasts, could be reprogrammed into pluripotent cells through the expression of a set of transcription factors, led to studies that examined whether fibroblasts could also be reprogrammed directly into cardiomyocytes (Takahashi and Yamanaka, 2006). This strategy is intriguing because it would utilize the cells responsible for fibrotic scar formation as a source of new cardiomyocytes. A combination of four factors known to play critical roles in cardiogenesis, Gata4, Mef2c, Tbx5, and Hand2, were subsequently identified to be able to induce mouse cardiac fibroblasts to take on characteristics of cardiomyocytes (Ieda et al., 2010; Qian et al., 2012). However, significant challenges that must be overcome include low reprogramming efficiency and immature maturation state of induced cardiomyocytes (Mohamed et al., 2017).

Proliferation of endogenous cardiomyocytes

During embryonic development, proliferation of cardiomyocytes contributes to the growth of the heart, but soon after birth, cardiomyocytes of the mammalian heart exit the cell cycle and switch to a hypertrophic mechanism of growth (Li et al., 1996; Oparil et al., 1984). A final approach to cardiac regeneration is based on the premise of developing therapies that reactivate the proliferation of endogenous cardiomyocytes to regenerate damaged tissue. This approach sets the foundation for the research presented in this dissertation.

1.3 PROLIFERATION AND REGENERATION IN THE HEART

Accumulating evidence has shown that in certain contexts, the heart is capable of regeneration through the proliferation of endogenous cardiomyocytes. A number of lower vertebrate and amphibian species, including zebrafish and newt, can fully regenerate myocardium after experimental injuries as severe as apical resection (Oberpriller and Oberpriller, 1974; Poss et al., 2002). Subsequent experiments utilized cardiomyocyte-specific cmlc2a-Cre-Ert2 lineage tracing in the zebrafish heart to show that the formation of new myocardium can be attributed to the proliferation of pre-existing cardiomyocytes (Kikuchi et al., 2010; Jopling et al., 2010). During regeneration, cardiomyocytes were observed to break down their sarcomere structure and express genes involved in the cell cycle but did not appear to undergo extensive dedifferentiation.

Furthermore, the mammalian heart displays a robust regenerative capacity during embryonic development (Drenckhahn et al., 2008; Sturzu et al., 2015). The murine heart retains this ability through the early postnatal period (Porrello et al., 2011). In response to apical resection of the heart at postnatal day 1, α-MHC-MerCreMer lineage traced cardiomyocytes entered the cell cycle and were observed to disassemble the sarcomere structure, mirroring the regenerative response observed in the zebrafish. However, cardiomyocytes were not able to mount a regenerative response when the injury occurred at postnatal day 7. This loss of regenerative response is concurrent with cardiomyocyte cell cycle exit during the first week after birth. The neonatal mouse heart responds similarly to an experimental injury model of myocardial infarction (Haubner et al., 2012).

Finally, several intriguing studies have been published noting the capacity of the neonatal human heart to fully recover after infarction. In one case study, a newborn presented with thrombotic occlusion of the left anterior descending artery within hours of birth (Haubner et al., 2016). High serum levels of troponin T signified the death of cardiomyocytes, and the child continued to show severe impairment of cardiac function in the days immediately following thrombolysis and re-establishment of coronary blood flow. However, by six weeks later, the child had regained complete cardiac function and showed no signs of injury. In fact, children as old as twelve have shown complete recovery of cardiac function after myocardial infarction (Celermajer et al., 1991).

While the regenerative ability of the heart appears to be lost over both evolutionary and developmental time, the possibility of reactivating the regenerative potential of the mammalian heart is supported by studies that show that a low level of cardiomyocyte turnover does occur during the lifetime of both the mouse and human (Mollova et al., 2013; Senyo et al., 2013). One study took advantage of a spike in atmospheric levels of carbon-14 (^{14}C) during nuclear bomb tests during the cold war to age cardiomyocytes from deceased individuals (Bergmann et al., 2009). The investigators isolated cardiac troponin-positive cardiomyocytes by FACS, extracted DNA, and assessed levels of ^{14}C in individuals born before and after the increase in ^{14}C. They then developed a mathematical model that suggested that new cardiomyocyte turnover does occur, albeit at a low rate, over the human lifetime. Taken together, these observations suggest that by understanding and modulating the mechanisms responsible for cardiomyocyte proliferation and regeneration, we could potentially accelerate the proliferation of cardiomyocytes for the regeneration of damaged tissue.

1.4 CARDIOMYOCYTE CELL CYCLE STUDIES

A large body of research has explored the possibility of experimentally manipulating the proliferative dynamics of cardiomyocytes. These studies have largely focused on modulating cell cycle regulators or growth factor pathways (Agah et al., 1997; Engel et al., 2005; Liao et al., 2001; MacLellan et al., 2005; Poolman et al., 1999; Soonpaa et al., 1997; Xiao et al., 2001). Several more recent studies have focused on the

Hippo pathway (Heallen et al., 2013; Leach et al., 2017; Tian et al., 2015; Xin et al., 2013). A number of groups have reported increased cardiomyocyte proliferation, but the responses largely do not appear to be robust enough for meaningful regeneration after injury. However, these studies have revealed valuable insights into cardiomyocyte proliferation that have guided ongoing research in the field, including the work presented in this dissertation.

Cardiomyocytes face multiple barriers to cell cycle progression

Several early studies used transgenic models to modulate the expression of individual cell cycle regulators and observed that in response, cardiomyocytes underwent additional partial rounds of the cell cycle (Liao et al., 2001; Poolman et al., 1999). Overexpression of cyclin D1 or c-Myc each resulted in DNA synthesis and increased polyploidy and multinucleation in cardiomyocytes of the adult heart (Soonpaa et al., 1997; Xiao et al., 2001). Overexpression of cyclin D1 also resulted in increased cardiomyocytes size (hypertrophy). These observed phenotypes can result from premature cell cycle exit (Figure 1.1) and suggest that cardiomyocytes underwent additional rounds of DNA synthesis in response to stimuli but faced additional obstacles that impeded completion of the cell cycle. Therefore, it appears that cardiomyocytes experience barriers to division at multiple different stages of the cell cycle. These observations also raise significant challenges in assessing cardiomyocyte proliferation.

Standard measures of cell proliferation, including measurements of BrdU incorporation and stains for phosphorylated Histone H3 and Aurora B kinase, do not definitively mark proliferating cardiomyocytes but instead only reveal how far into the cell cycle a cardiomyocyte has progressed at a given time. This has remained a significant challenge in the field. While no available technique conclusively shows cardiomyocyte proliferation, the most rigorous assessments use a combination of BrdU incorporation assays, cell cycle marker stains, and either quantification of increased cardiomyocyte number in the heart or time-lapse imaging of dividing cardiomyocytes (Figure 1.2).

Proliferation and differentiation are linked

Later studies identified experimental strategies that led to more robust activation of the cardiomyocyte cell cycle and, in doing so, also revealed new challenges. Hearts deficient in pocket proteins Rb and p130 showed strong upregulation of several key cell cycle regulators and contained cardiomyocytes positive for BrdU and phosphorylated histone H3. However, these changes were accompanied by the expression of the immature isoform of the myosin heavy chain (MHC) gene and decreased cardiac function (MacLellan et al., 2005). Work from our lab showed that transgenic overexpression of the microRNA family miR-302/367 activates the cardiomyocyte cell cycle at least in part through repression of the Hippo pathway (Tian et al., 2015). However, prolonged reactivation of the cell cycle also led to the expression of genes associated with immature

cardiomyocytes and a disorganized sarcomere structure. These indications of dedifferentiation were accompanied by decreased cardiac function. In contrast, transient delivery of miR-302/367 mimics resulted in improved cardiac function after injury. In addition to the challenges they raise, these results also suggest that regulation of proliferation and maturation of cardiomyocytes are closely linked.

Cardiomyocytes appear to lose competency to respond to proliferative stimuli

Studies have shown that the cardiomyocyte cell cycle can be reactivated in response to several different experimental strategies. However, reported measurements of DNA synthesis by BrdU incorporation suggest that an extremely limited proportion of adult cardiomyocytes undergo even early stages of the cell cycle in response to these stimuli (Figure 1.3). In several studies, however, early neonatal cardiomyocytes were shown to respond more robustly to stimuli. Treatment of postnatal day 2 rat cardiomyocytes with a combination of FGF1 and a p38 MAP kinase inhibitor resulted in BrdU incorporation in approximately 80% of treated cardiomyocytes compared to 5% of untreated cardiomyocytes. In contrast, when adult cardiomyocytes were treated with the same conditions, approximately 4% of cells incorporated BrdU (Engel et al., 2005). Similar trends resulted from stimulation with growth factor neuregulin1 or transgenic overexpression of receptor tyrosine kinase ErbB4 (Bersell et al., 2009). These

observations suggest that events occur during the neonatal period that act to shut off the ability of cardiomyocytes to respond to proliferative stimuli.

Mononucleated cardiomyocytes retain increased proliferative competency

Two studies reported that a higher proportion of mononucleated cardiomyocytes (MoNucs) than binucleated cardiomyocytes (BiNucs) reactivate the cell cycle in response to proliferative stimuli (Bersell et al., 2009; Kuhn et al., 2007) (Figure 1.3). Our lab also observed this trend as a result of adenoviral-mediated delivery of the miR-302/367 transcript to adult rat cardiomyocytes in vitro. While MoNucs comprise a small fraction of adult rat cardiomyocytes, they were highly overrepresented in the cardiomyocytes that responded to miR-302/367 (Figure 1.4). These data suggest that though mature cardiomyocytes largely appear to lack competency to respond to proliferative stimuli, MoNucs may represent a subset of cardiomyocytes with increased proliferative competency. Moreover, these observations suggest that mononucleated and binucleated cardiomyocytes could provide a biological model with which to interrogate loss of proliferative competency.

The insights gained from these studies begin to piece together a picture of the rules and roadblocks that govern cardiomyocyte proliferation. They also bring to light many intriguing new questions. The research presented in this dissertation aims to

address some of these questions: 1) What events are responsible for the loss of proliferative competency during the postnatal maturation period? 2) What are the molecular differences underlying the distinct proliferative responses of MoNucs and BiNucs? 3) Do differences in the maturation processes undergone by MoNucs and BiNucs leave them differentially competent to respond to proliferative stimuli?

The remainder of this chapter will discuss our current understanding of the relationship between binucleation, the postnatal maturation period, and the loss of proliferative competency.

1.5 BINUCLEATION OF CARDIOMYOCYTES

During embryonic development, almost all cardiomyocytes are mononucleated, which correlates with ongoing cardiomyocyte proliferation to drive organ growth. Soon after birth, cardiomyocytes of the mammalian heart undergo a transition period associated with cell cycle exit and maturation. During cell cycle exit, karyokinesis (nuclear division) and cytokinesis (cytoplasmic division) become uncoupled in the murine heart. Cardiomyocytes undergo a final round of DNA synthesis and nuclear division but do not complete cytokinesis (Li et al., 1996). These events occur between postnatal days 4 and 7 and result in a high percentage of binucleated cardiomyocytes (Soonpaa et al., 1996). After this period, only a small minority of cardiomyocyte remain mononucleated. Between postnatal days 2 and 4, cardiomyocytes appear to lose their ability to fully

disassemble myofibrils during cell division and this has been proposed to be responsible for failed cytokinesis and subsequent binucleation (Li et al., 1996). However, a different study reported successful myofibril disassembly and instead suggested that failed cytokinesis is the result of the mis-localization of the cytokinesis protein anillin (Engel et al., 2006). The study suggested that improper localization of anillin results in the disfunction of the actomyosin contractile ring responsible for carrying out cytokinesis. Therefore, the events responsible for the binucleation of cardiomyocytes remain incompletely resolved.

In recent years, new reports have provided further evidence that MoNucs retain an increased potential to proliferate and to contribute to cardiac regeneration. Patterson *et al*. characterized 120 different inbred mouse strains and found that the percentage of diploid MoNucs in the heart varied from approximately 2% to 10%. The investigators took advantage of this natural variation to show a positive correlation between the percentage of MoNucs in the heart and the number of cells that re-enter the cell cycle after injury as well as functional repair of the heart after injury (Patterson et al., 2017). Another intriguing study used the zebrafish as a model, which retains a lifelong capacity for cardiac regeneration and contains almost solely MoNucs under physiological conditions. The authors of this study expressed a dominant-negative Ect2 in zebrafish cardiomyocytes to induce polyploidy and binucleation and showed that it impaired the heart's ability to regenerate after injury (Gonzalez-Rosa et al., 2018). Despite these

intriguing observations, there have been no studies directly comparing MoNucs and BiNucs in the mammalian heart, and the molecular basis for their distinct proliferative responses remains unclear.

1.6 REGULATION OF CELL CYCLE EXIT

Cell cycle exit and maturation during the neonatal period are accompanied by large scale, programmatic shifts in the gene expression profile of cardiomyocytes. Over late embryonic development and through the postnatal period, a multitude of genes involved in the cell cycle are downregulated, while those associated with cardiomyocyte-specific processes are upregulated (Uosaki et al., 2015). The onset of cell cycle exit and maturation can be altered to various degrees in response to experimental manipulation of many different pathways that include Hippo, Rb/E2f, FGF, Myc, and Cdks/Cyclins (Engel et al., 2005; MacLellan et al., 2005; Poolman et al., 1999; Tian et al., 2015; Xiao et al., 2001; Xin et al., 2011). Therefore, it has remained a significant challenge to determine the relative contributions of these different pathways to cell cycle exit, binucleation, and loss of proliferative competency.

Cell cycle exit and maturation are tightly coupled to birth and have been proposed to occur at least in part as a response to exposure to oxygen. The switch from a hypoxic environment to an oxygen-rich environment results in reactive oxygen species

production, which in turn activates a DNA damage response pathway (Puente et al., 2014). It is this pathway that is thought to potentially initiate cell cycle exit and mitochondrial biogenesis. In contrast, there is also evidence that pathways related to the cell cycle and maturation begin to change expression levels during late embryonic development (Uosaki et al., 2015). Therefore, the upstream events that initiate cell cycle exit and maturation of cardiomyocytes remain incompletely resolved.

1.7 CARDIOMYOCYTE MATURATION

During the neonatal period, cell cycle exit and binucleation of cardiomyocytes are accompanied by structural and metabolic changes that leave the heart better prepared to meet the high physical and metabolic demands placed on it over the mammalian lifetime. These changes may also not be conducive to cell division.

The sarcomere is the contractile unit of the cardiomyocyte and is composed of actin and myosin along with a large number of proteins involved in scaffolding and mechanotransduction. Repeating sarcomere units comprise myofibrils, which must break down, at least in part, for cell division to occur (Ahuja et al., 2004). During neonatal cardiomyocyte maturation, the sarcomere structure becomes more highly organized and rigid, which allows it to generate more force (Jacot et al., 2010; Murphy, 1996; Siedner et al., 2003). Changes in sarcomere organization and density are reflections of the

upregulation and expression of alternate isoforms of sarcomere components (Lahmers et al., 2004; Saggin et al., 1989). While myofibrils were observed to disassemble during cell division in 2-day-old rat cardiomyocytes, they do not do so completely in cardiomyocytes from 4-day-old rats (Li et al., 1996; Li et al., 1997). During cardiac regeneration in zebrafish, proliferating cardiomyocytes transiently break down myofibrils (Jopling et al., 2010). Therefore, the inability of the sarcomere structure to break down in mammalian cardiomyocytes is thought to be a potential barrier to the completion of cytokinesis in cardiomyocytes and to contribute to the formation of BiNucs during the postnatal period.

During embryonic development, cardiomyocytes utilize glycolytic metabolism for energy. Within days after birth, there is a dramatic decrease in glycolysis as cardiomyocytes switch to instead utilize fatty acid β-oxidation as the primary energy source (Lopaschuk and Jaswal, 2010). This switch is accompanied by a marked increase in mitochondrial mass and ultrastructural rearrangements that ensure myofibrils are continuously able to receive a high supply of ATP (Piquereau et al., 2010). Interestingly, rapidly proliferating cells, including cancer cells, have been found to rely primarily on glycolytic metabolism (Warburg, 1925). It has been proposed that a proliferating cell may require glycolysis because glycolytic intermediates provide the raw material for the biosynthesis of nucleic acids, proteins, and lipids necessary to make a new cell (Lunt and Vander Heiden, 2011). It is currently unknown whether a limited capacity for glycolytic

metabolism in mature cardiomyocytes plays any role in restricting their ability to re-enter the cell cycle.

1.8 MAINTENANCE OF THE TERMINALLY DIFFERENTIATED STATE

Widespread epigenetic changes occur during cardiomyocyte maturation and are thought to maintain the mature state of cardiomyocytes after the neonatal period. DNA methylation increases globally in cardiomyocytes over the neonatal period (Kou et al., 2010). Furthermore, ATAC-seq has shown that promoters of genes associated with the cell cycle become less accessible over cardiomyocyte maturation, while those associated with sarcomere structure and metabolism become more accessible (Quaife-Ryan et al., 2017). Genes that regulate DNA synthesis have been shown to acquire H3K9me3 and H3K27me3 histone modifications and CpG methylation changes over cardiomyocyte maturation (Gilsbach et al., 2018; Kou et al., 2010). While these changes are known to occur over maturation, their role in inhibiting cardiomyocyte proliferation and regeneration remains an area of active research.

1.9 HYPOTHESIS AND APPROACH

The research presented in this dissertation aims to further our understanding of the mechanisms responsible for the loss of proliferative competency of cardiomyocytes. We sought to gain insight into how the cell cycle is permanently shut off to better understand

how we might turn it back on. We have employed mononucleated and binucleated cardiomyocytes as a biological model of differential proliferative competency. The two cardiomyocyte subsets diverge during a neonatal period associated with cell cycle exit, maturation, and loss of regenerative capacity. We hypothesized that differences in the maturation processes undergone by mononucleated and binucleated cardiomyocytes leave them differentially primed to respond to proliferative stimuli. To address this hypothesis, we characterized the transcriptional differences between the two subsets across developmental time.

Figure 1.1 The Cardiomyocyte Cell Cycle

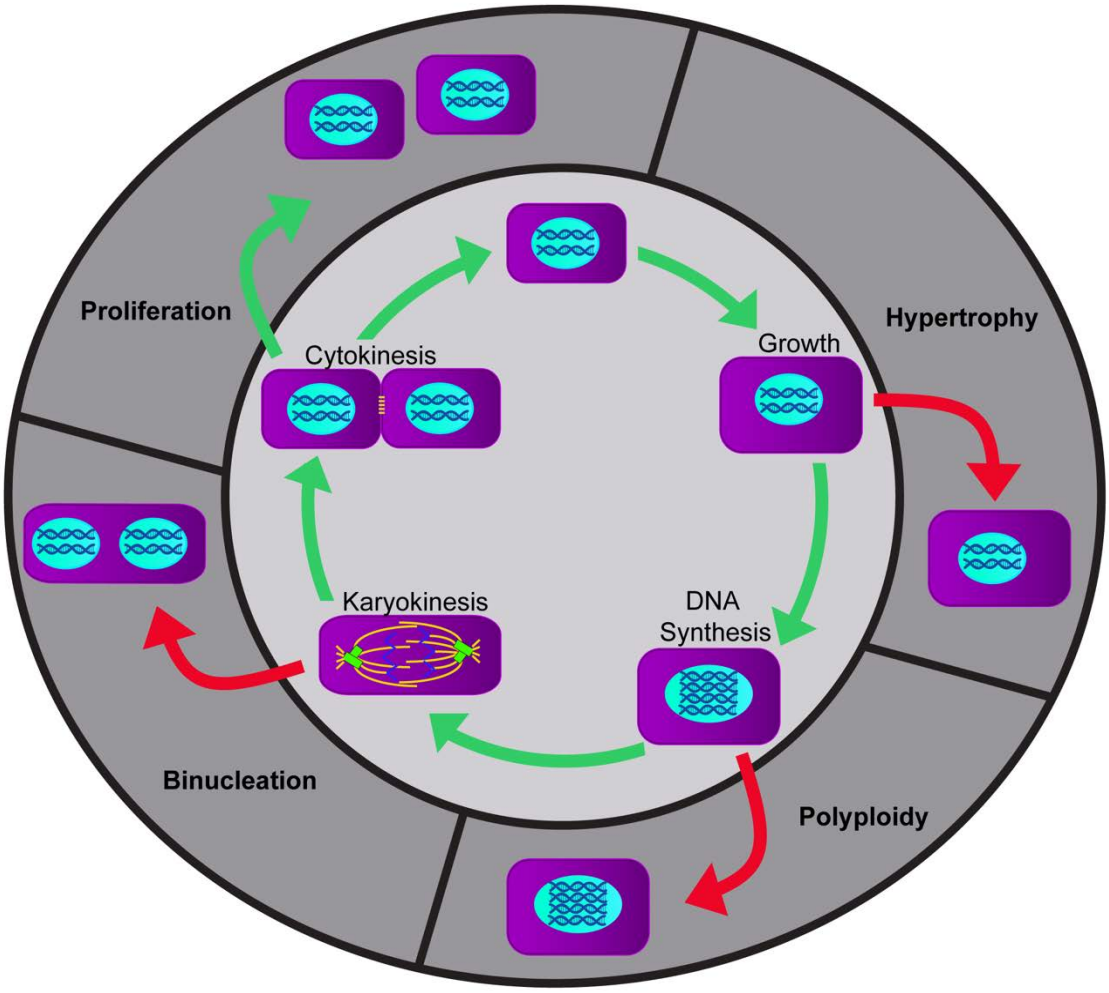

Figure 1.1 The Cardiomyocyte Cell Cycle

Cardiomyocytes can progress partially through the cell cycle and exit prematurely. Cells that exit the cell cycle during G1 may be hypertrophic. Cells that undergo DNA synthesis but do not complete mitosis become polyploid. Cells also may begin mitosis but exit the cell cycle between karyokinesis and cytokinesis. This results in multinucleated cells. Cardiomyocytes can exist in hypertrophic, polyploid, and multinucleated states under physiological conditions but also as a result of pathological conditions or in response to experimental stimuli.

Figure 1.2 Reports of cell cycle progression in response to proliferative stimuli

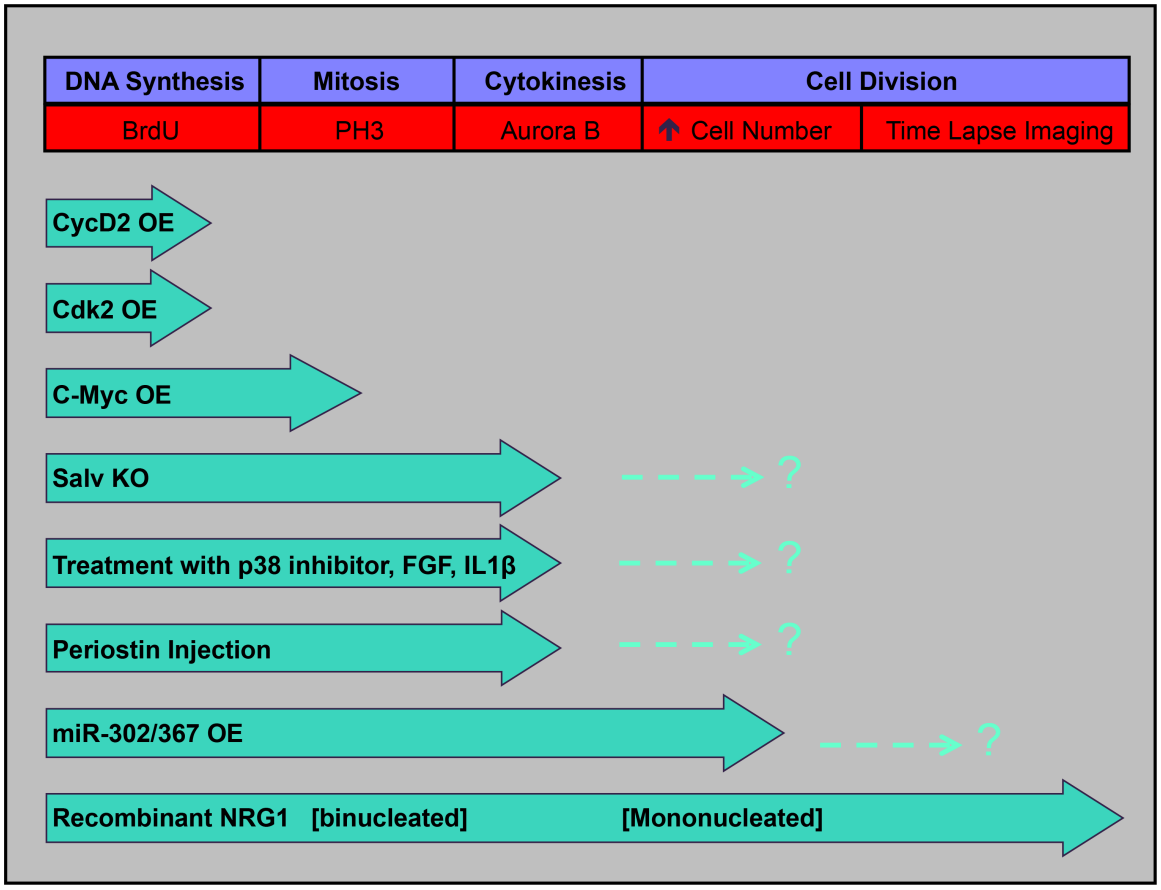

Figure 1.2 Reports of cell cycle progression in response to proliferative stimuli

Cardiomyocytes can partially progress through the cell cycle before prematurely exiting. Therefore, the data shown here does not show true cardiomyocyte proliferation but instead how far in the cell cycle the cardiomyocyte has been able to progress at a given time. The furthest point in the cell cycle reported for different pro-proliferative stimuli are shown. (Bersell et al., 2009; Engel et al., 2005; Heallen et al., 2013; Kuhn et al., 2007; Lavine et al., 2005; Liao et al., 2001; Pasumarthi et al., 2005; Soonpaa et al., 1996; von Gise et al., 2012; Xiao et al., 2001)

Figure 1.3 Reports of DNA synthesis in response to proliferative stimuli

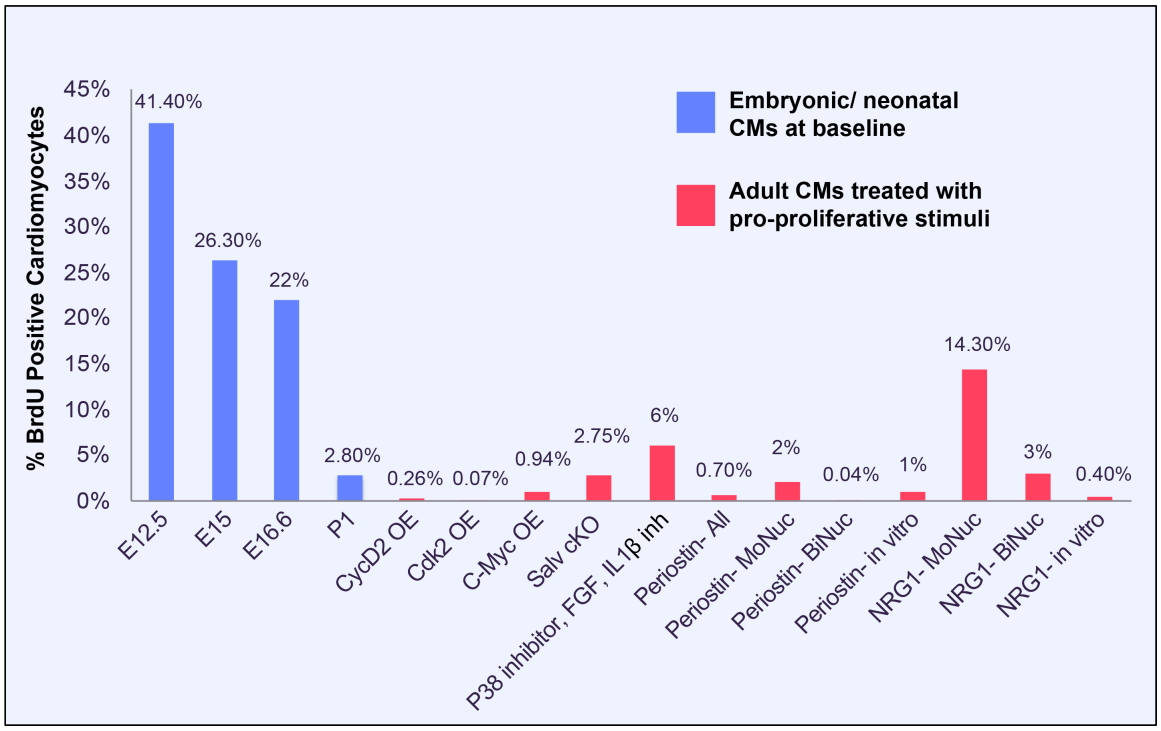

Figure 1.3 Reports of DNA synthesis in response to proliferative stimuli

Reported measures of BrdU incorporation in adult cardiomyocytes in response to proliferative stimuli are shown in pink. Typical percentages of cycling cardiomyocytes in the embryonic heart reported in the literature are shown in purple for comparison. Data shows that the majority of cardiomyocytes fail to undergo even early stages of the cell cycle in response to proliferative stimuli. Two studies report that a higher percentage of mononucleated cardiomyocytes than binucleated cardiomyocytes reactivate the cell cycle. (Bersell et al., 2009; Engel et al., 2005; Heallen et al., 2013; Kuhn et al., 2007; Lavine et al., 2005; Liao et al., 2001; Pasumarthi et al., 2005; Soonpaa et al., 1996; von Gise et al., 2012; Xiao et al., 2001)

Figure 1.4 MoNucs are overrepresented in cardiomyocytes that respond to miR-302/367

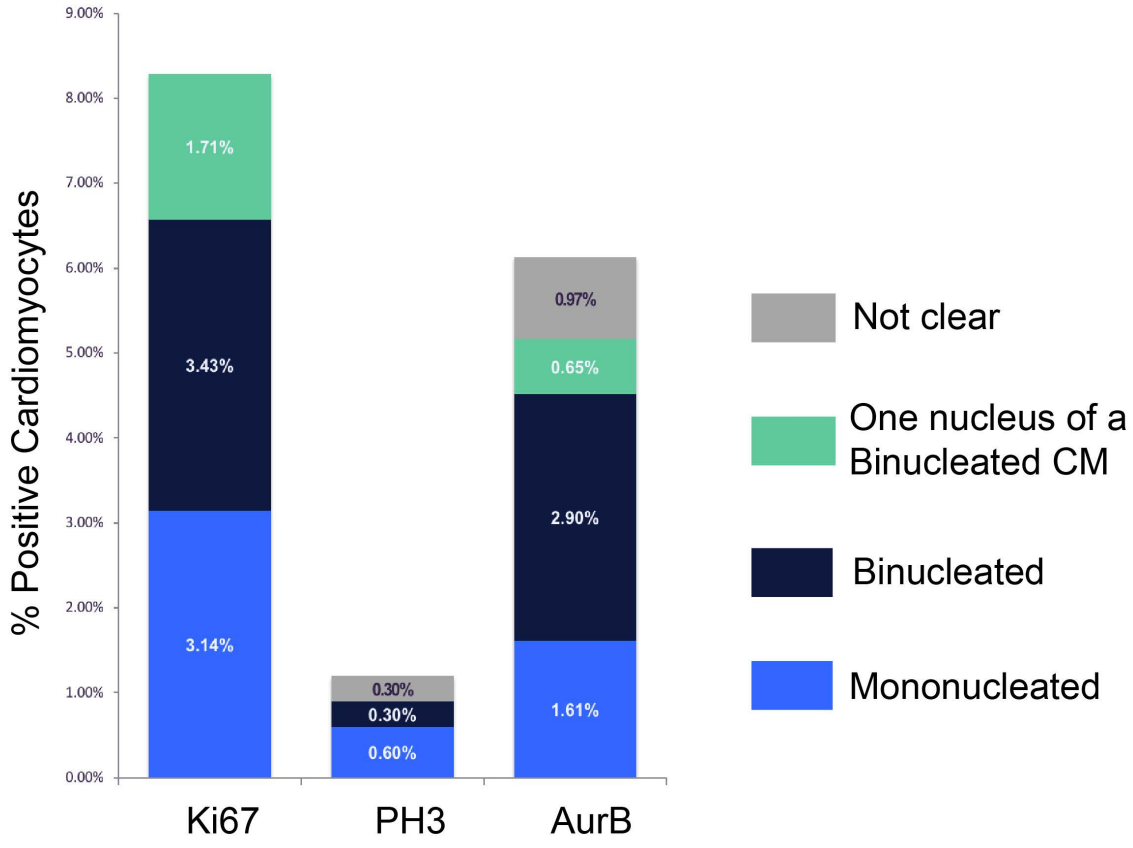

Figure 1.4 MoNucs are overrepresented in cardiomyocytes that respond to miR-302/367

Measures of cell cycle activation by immunostaining 6d after in vitro adenoviral mediated infection of the miR-302/367 transcript in freshly isolated rat cardiomyocytes. Percentages are reported as cell staining positive for the specified cell cycle reporter out of total cells staining positive for cardiomyocyte marker Sarcomeric α-actinin. Taking into account that only ~10% of adult murine cardiomyocytes are mononucleated, this data shows MoNucs are overrepresented in the cardiomyocytes that respond to proliferative stimuli.

CHAPTER 2: DIRECT COMPARISON OF MONONUCLEATED AND BINUCLEATED CARDIOMYOCYTES REVEALS MOLECULAR MECHANISMS UNDERLYING DISTINCT PROLIFERATIVE COMPETENCIES

2.1 SUMMARY

Several reports have demonstrated that mononucleated (MoNuc) cardiomyocytes are more responsive to pro-proliferative stimuli than are binucleated (BiNuc) cardiomyocytes. However, techniques to isolate and characterize these two different cardiomyocyte populations have been lacking. To address whether the developmental divergence of MoNucs and BiNucs contributes to their differential response to proliferative stimuli, we developed a novel strategy to separate MoNuc and BiNuc cardiomyocytes using fluorescence-activated cell sorting (FACS). We assessed the transcriptional differences between these subsets of cardiomyocytes across late development and in the adult. These data revealed that during the neonatal period, binucleation is associated with the silencing of genes that permit the onset of DNA synthesis, specifically those that are targets of the E2f transcription factor family, and the upregulation of a set of genes involved in cardiomyocyte maturation. Remnants of the differences between MoNucs and BiNucs established during the neonatal period remain at the adult stage. Furthermore, we showed that Rb is required for the down-regulation of E2f target genes that we observed to occur.

2.2 MONONUCLEATED AND BINUCLEATED CARDIOMYOCYTES CAN BE SEPARATED BY FACS

We sought to characterize transcriptional differences between MoNuc and BiNuc cardiomyocytes during maturation from late embryonic development through adulthood. Single-cell suspensions were prepared from hearts at the indicated timepoints to be sorted by FACS (Figure 2.1A). A wide nozzle was used to accommodate the large size of mature cardiomyocytes. A wide nozzle also subjects the cardiomyocytes to lower shear stress than is typical for FACS (Shapiro, 1985). Ventricular cardiomyocytes were lineage labeled with $Mlc2v^{cre}$:$R26R^{EYFP}$, and nuclei were stained with Vybrant™ DyeCycle™ DNA dye. The intensity of the fluorescent signal emitted by this dye is proportional to the DNA quantity. The dye is used to assess DNA content and ploidy of nuclei by FACS (Patterson et al., 2017). Cells were gated on EYFP presence then determined to be MoNucs or BiNucs by a strategy that combines the use of DyeCycle™ dye with the concept behind doublet discrimination (Figure 2.1B). Doublet discrimination is used in FACS analysis to exclude instances where two cells are stuck together and are therefore characterized as a single event. Doublet discrimination takes into account the width (time), and the height (voltage intensity) of the signal produced and assumes that two cells will produce a signal of greater width than a single cell, while the height of the signal will remain the same. We utilized a similar metric to distinguish BiNucs from MoNucs. Nucleation was gated on the height and width of the fluorescent signal produced by 405nm laser excitation of DyeCycle™ dye. (Figure 2.2A-C). The nuclei of

BiNucs produced a signal of equal intensity to that produced by diploid MoNucs but of greater width. MoNucs with increased voltage intensity, presumed to be polyploid or undergoing DNA synthesis, were excluded. Since the size and shape of cardiomyocytes change over maturation, each timepoint required tailored gating parameters. These parameters were empirically fine-tuned to maximize enrichment by sorting cells onto microscope slides for visualization of nucleation (Figure 2.2D-I). The relative percentages of MoNucs and BiNucs collected at each timepoint faithfully reflects the developmental switch to BiNucs being the predominant cardiomyocyte subtype, and agree with reported percentages of MoNucs and BiNucs over cardiomyocyte maturation (Ikenishi et al., 2012). This methodology resulted in greater than 70% enrichment of either MoNucs or BiNucs at the E18.5 timepoint and greater than 90% enrichment at the P7 and adult timepoints (Figure 2.2J-L). We quantified the viability of sorted cardiomyocytes by propidium iodide (PI) staining. At each timepoint, >97% of cells remained negative for PI after being sorted (Figure 2.3A-B). Finally, we expanded the application of our FACS strategy to separate adult MoNucs and BiNucs without the requirement of a lineage marker (Figure 2.4A). We reasoned that a long rod-shaped cardiomyocyte would produce a wider light scatter than a smaller round non-myocyte, similar to our gating for two nuclei versus one. To quantify the ability of this strategy to identify cardiomyocytes accurately, we gated lineage traced cells on the width of side scatter and then backgated on YFP fluorescence, showing that 99.1% of cells identified are cardiomyocytes by their YFP expression (Figure 2.4B-C). Importantly, we were able

to separate MoNucs and BiNucs by their distinct light scatter with equal success rates using this strategy (Figure 2.4D-E). Together, the techniques described here allowed us to isolate highly enriched populations of lineage labeled MoNuc and BiNuc cardiomyocytes from E18.5, P7, and adult mice to assess changes in gene expression during cardiomyocyte maturation.

2.3 BINUCLEATION IS ACCOMPANIED BY A SWITCH FROM A PROLIFERATION- TO MATURATION-ASSOCIATED GENE EXPRESSION PROGRAM

To characterize transcriptional differences between MoNucs and BiNucs over the neonatal maturation period, we sorted MoNuc and BiNuc cardiomyocyte populations and performed RNA-seq analysis. The Principal Component Analysis (PCA) shows that at each timepoint, MoNucs and BiNucs are transcriptionally distinct with the primary and secondary components accounting for 76.2% and 9.6% respectively of the variance across all of the samples (Figure 2.5A). At E18.5, BiNucs were enriched for genes involved in cell division, including several genes known to be involved in cytokinesis (Figure 2.6). This data suggests that at this timepoint, cardiomyocytes identified as BiNucs may have still been undergoing or attempting to undergo cytokinesis. The RNA-seq data revealed that MoNucs and BiNucs exhibit the most statistically significant differences in gene expression at P7. To further characterize the set of genes differentially expressed between P7 MoNucs and BiNucs, we examined their expression levels across

all samples. (Figure 2.7A). We observed that the expression of this set of genes also changes significantly between the embryonic and adult timepoints. The genes upregulated in P7 MoNucs tend to be more highly expressed in both embryonic cardiomyocyte populations compared to adult cardiomyocytes, whereas the genes upregulated in P7 BiNucs tend to be enriched in both adult cardiomyocyte populations versus embryonic cardiomyocytes. Gene set enrichment analysis (GSEA) showed that P7 MoNucs are enriched for genes involved in the cell cycle, especially those that are E2f targets and those involved in DNA synthesis (Figure 2.7B, Figure 2.8A-B, Table 2.1). In contrast, P7 BiNucs are enriched for genes involved in cardiomyocyte maturation processes, including sarcomere organization and a switch to fatty acid oxidative metabolism (Figure 2.7B, Figure 2.8C-D, Table 2.2). Together, this data indicates that during the postnatal period, cardiomyocyte binucleation is accompanied by the termination of the fetal gene expression program, including genes required for proliferation, in exchange for activation of the mature cardiomyocyte gene expression program.

2.4 BINUCLEATED CARDIOMYOCYTES AT P7 TURN OFF E2F TARGET GENE EXPRESSION REQUIRED FOR G1/S PHASE TRANSITION

Transcriptome analysis revealed that at P7, binucleation is accompanied by the termination of a gene expression program closely associated with regulating the onset of proliferation. To gain insight into which transcription factors may be involved in

regulating the apparent switch in transcription program, we analyzed the promoters of differentially expressed genes at P7 for the enrichment of DNA binding sites and associated transcription factors. This analysis revealed that binucleation is accompanied by down-regulation of targets of the E2f transcription factor family, whereas genes upregulated in P7 BiNucs are targets of the Ppara, Esrra, Mef2, and Myod transcription factors (Figure 2.9A). The E2f transcription factor family is known to control the onset of DNA synthesis (Nevins, 1992). Our RNA-seq data shows that 54% of the top 50 down-regulated genes in P7 BiNucs are targets of E2f that are known to regulate the G1/S transition and onset of DNA synthesis (Figure 2.9B, C). This down-regulation occurs most dramatically between P7 MoNucs and BiNucs (Figure 2.10A). In addition to their target genes, four of the E2f family members, E2f1, E2f2, E2f7, and E2f8, were strongly down-regulated in P7 BiNucs (Figure 2.10B). These data demonstrate that DNA synthesis and onset of the cell cycle is dramatically down-regulated in association with binucleation in P7 cardiomyocytes, through silencing of E2f target genes.

2.5 ADULT MONONUCLEATED AND BINUCLEATED CARDIOMYOCYTES RETAIN DIFFERENCES ESTABLISHED DURING NEONATAL MATURATION

To determine whether differences between P7 MoNucs and BiNucs remained in adult cardiomyocytes, we compared the transcriptional profiles of MoNucs and BiNucs from adult hearts. Transcriptionally, these cardiomyocyte subsets are quite similar, with only three differentially expressed genes with an FDR < 0.05 (Figure 2.11A). However,

two of these genes, Necdin and Cenpf, are known to be involved in the regulation of E2f/Rb signaling (Papadimou et al., 2005; Taniura et al., 1998). 456 genes had a non-adjusted p-value < 0.05 (Figure 2.11B). GSEA of these genes revealed enrichment of categories related to those that are differentially expressed between P7 MoNucs and BiNucs (Figure 2.11C, Table 2.3). While adult MoNucs are enriched for genes involved in DNA synthesis and G2 phase of the cell cycle, adult BiNucs are enriched for genes involved in fatty acid oxidation. Furthermore, several of the most highly downregulated E2f target genes in the P7 BiNucs remain downregulated in the Adult BiNucs (Figure 2.11D). Together, this data shows that adult MoNucs and BiNucs retain remnants of transcriptional differences established during the neonatal maturation period.

To further examine differences between adult MoNucs and BiNucs, we performed transmission electron microscopy studies on sorted cardiomyocytes. We observed that adult BiNucs have a significantly higher density and buildup of glycogen granules surrounding the mitochondria than do MoNucs (Figure 2.12A-B). Glycogen granules are a stored energy source that is depleted when used to drive glycolytic metabolism (Prats et al., 2018; Schneider et al., 2014). This observation suggests that metabolic differences exist between adult MoNucs and BiNucs. One possible explanation for this observation is that diploid adult MoNucs may utilize glycolytic metabolism more readily than BiNucs and are therefore not able to maintain stores of excess glycogen. This would be consistent with the switch away from glycolytic metabolism that occurs during cardiomyocyte

maturation and the oxidative metabolism gene expression profile that we observed to be enriched in BiNucs at the P7 and adult stages. These data further support the concept that adult MoNucs and BiNucs retain remnants of differences established during the neonatal maturation period.

2.6 RB IS REQUIRED FOR DOWNREGULATION OF E2F TARGET GENES

E2f activity is known to be regulated by Rb, and this interaction can have temporary, as well as long term control over entry into S phase of the cell cycle (Harrington et al., 1998; Lundberg and Weinberg, 1998; Nevins, 1992). Previous work has shown that Rb family members are required for cell cycle exit of cardiomyocytes during the postnatal period (MacLellan et al., 2005). Furthermore, Rb recruits HP1-γ to H3K9me3 marks at a subset of E2f target genes to stably repress their expression during cardiomyocyte maturation (Sdek et al., 2011). Therefore, we sought to determine whether Rb is required for the repression of E2f target genes that we saw to be depleted in P7 BiNucs. We utilized a triple Rb family knockout mouse model, $Rb^{flox/flox};p130^{flox/flox};p107^{-/-}$ (Viatour et al., 2008) to determine the role of the Rb family in cardiomyocyte binucleation. Cardiomyocytes were isolated from P1 mice and infected with either adenoviral-Cre/GFP (TKO) or adenoviral-GFP (control) in vitro (Figure 2.13A). QPCR revealed strong downregulation of the Rb1 transcript in TKO cardiomyocytes (Figure 2.13B). We then quantified the percentage of GFP+ MoNucs and BiNucs in both control and TKO samples to determine whether Rb activity regulates the

onset of binucleation. There was no difference in the ratio of BiNucs to MoNucs between control and TKO cardiomyocytes (Figure 2.13C-D). QPCR revealed that TKO cardiomyocytes strongly upregulated E2f target genes whose expression are decreased in P7 BiNucs versus MoNucs (Figure 2.13E). In contrast, non-E2f targets were upregulated to a lesser degree in TKO cardiomyocytes (Figure 2.13E-F). Together this data suggests that Rb is required for down-regulation of E2f target genes in neonatal cardiomyocytes and that Rb mediated changes in E2f target expression are not responsible for the onset of binucleation.

Figure 2.1 Schematic of MoNuc and BiNuc sorting strategy

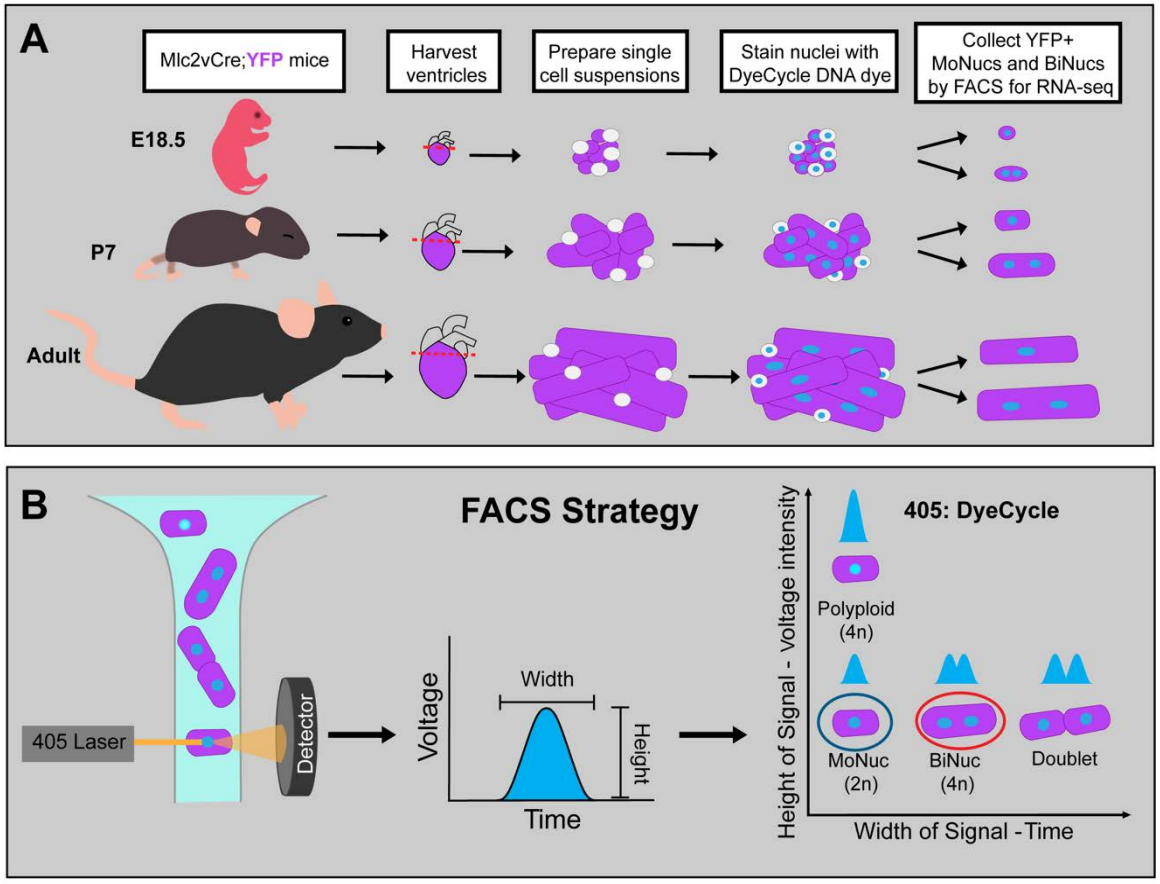

Figure 2.1 Schematic of MoNuc and BiNuc sorting strategy

(A) Schematic of experimental design to collect mononucleated (MoNucs) and binucleated (BiNucs) cardiomyocytes for RNA-sequencing analysis. Single-cell suspensions are isolated from the hearts of $Mlc2v^{cre}$:$R26R^{EYFP}$ mice at age E18.5, P7, and adult. Nuclei are stained with Vybrant™ DyeCycle™ DNA dye. Cardiomyocytes are identified by FACS as YFP+ and then sorted by nucleation. **(B)** Schematic of sorting strategy for separating MoNucs and BiNucs. As nuclei of cardiomyocytes pass the 405 nm laser, DyeCycle™ DNA dye is activated and produces a signal of which the width is proportional to the length of time the nuclei travel through the laser. Two nuclei (BiNucs) take longer to travel past the laser than one nucleus (MoNucs) and produce two overlapping signals, which are interpreted as a single signal of greater width. The height of the signal produced is proportional to DNA content per nucleus, allowing the separate gating of diploid and polyploid cells. MoNucs and BiNucs, cluster separately on a plot of width versus height of the 405 signal.

Figure 2.2 Results of FACS sorting to separate MoNucs and BiNucs

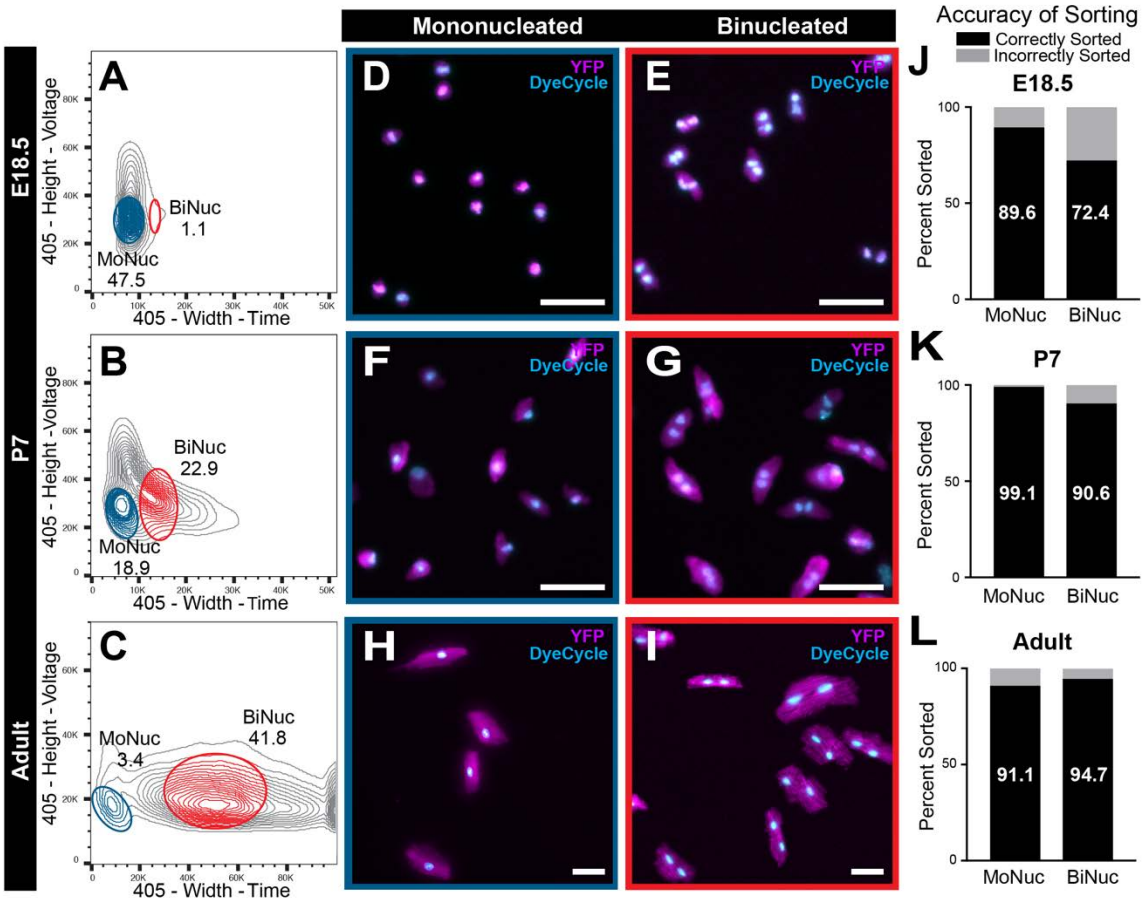

Figure 2.2 Results of FACS sorting to separate MoNucs and BiNucs

(A-C) Representative flow cytometry plots of the width versus height of the 405 channel. Gates used to sort E18.5 **(A)**, P7 **(B)**, and adult **(C)** MoNucs and BiNucs are shown. Mean percentages of total YFP+ cells that fall inside MoNuc or BiNuc gates are indicated. n=3 animals for each timepoint. **(D-I)** Cropped images of live Mlc2v^{cre}:R26R^{EYFP} MoNucs **(D, F, H,)** and BiNucs **(E, G, I)** sorted onto slides according to gates shown in **(A-C)**. Scale bar, 50 μm. **(J-L)** Percentages of cells correctly and incorrectly sorted into indicated groups as determined by slide images taken during sorts. >100 cells were counted for each group.

Figure 2.3 Validation and Viability of FACS methods

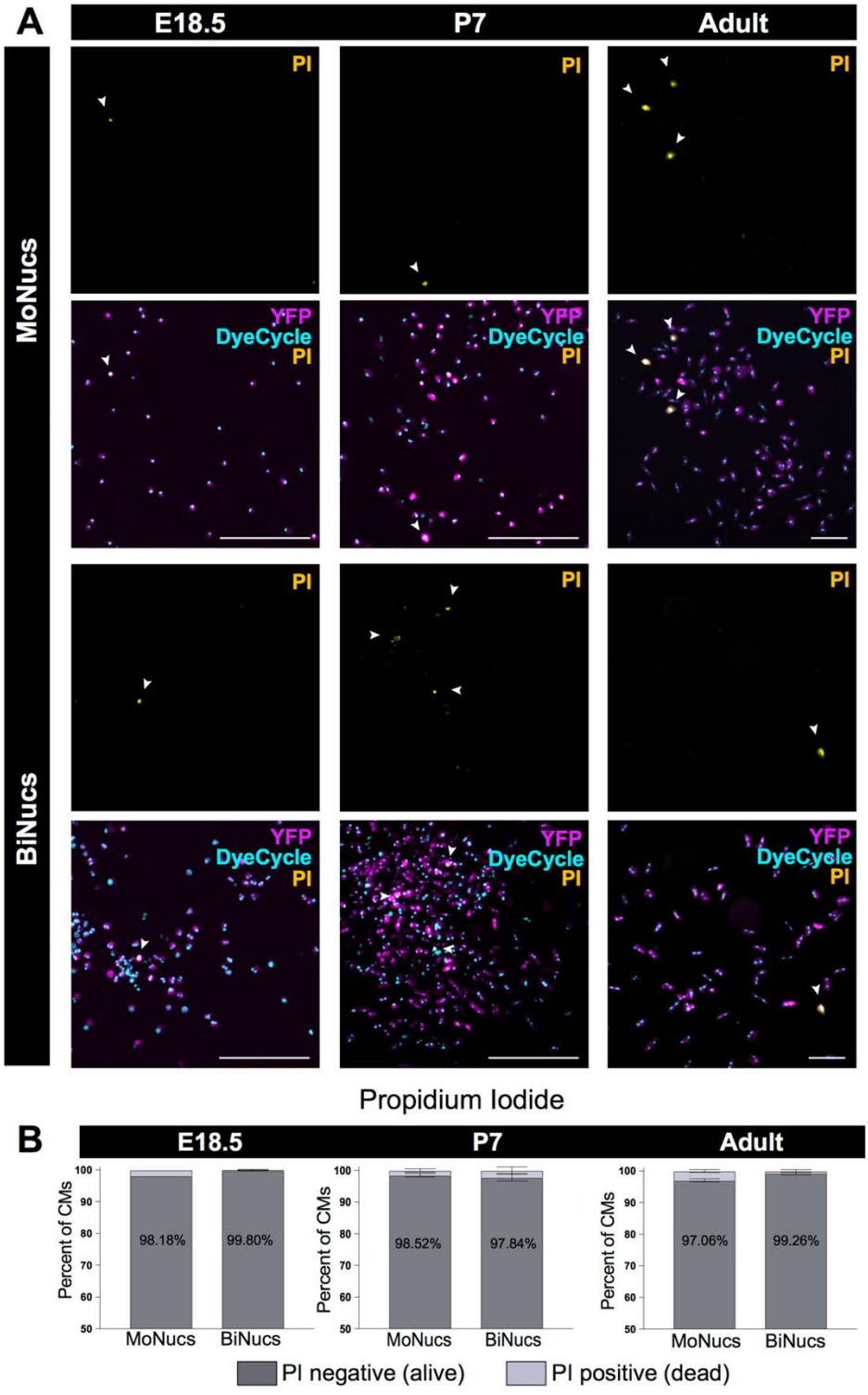

Figure 2.3 Validation and Viability of FACS methods

(A) Viability testing of FACS sorted cardiomyocytes. Cropped images of live E18.5, P7, adult Mlc2v^{cre}:R26R^{EYFP} MoNucs and BiNucs stained with Propidium Iodide. Cardiomyocytes gated on negative Propidium iodide staining were sorted onto slides according to gates shown in (Figure 2.1 A-C) and imaged to determine levels of cell death associated with the sorting process. Scale bar, 200 μm. (**B**) Quantification of percentages of cells staining positive and negative for Propidium iodide after FACS sorting. >100 cells were counted per group.

Figure 2.4 Expanded FACS strategy allows the sorting of cardiomyocytes without a lineage marker

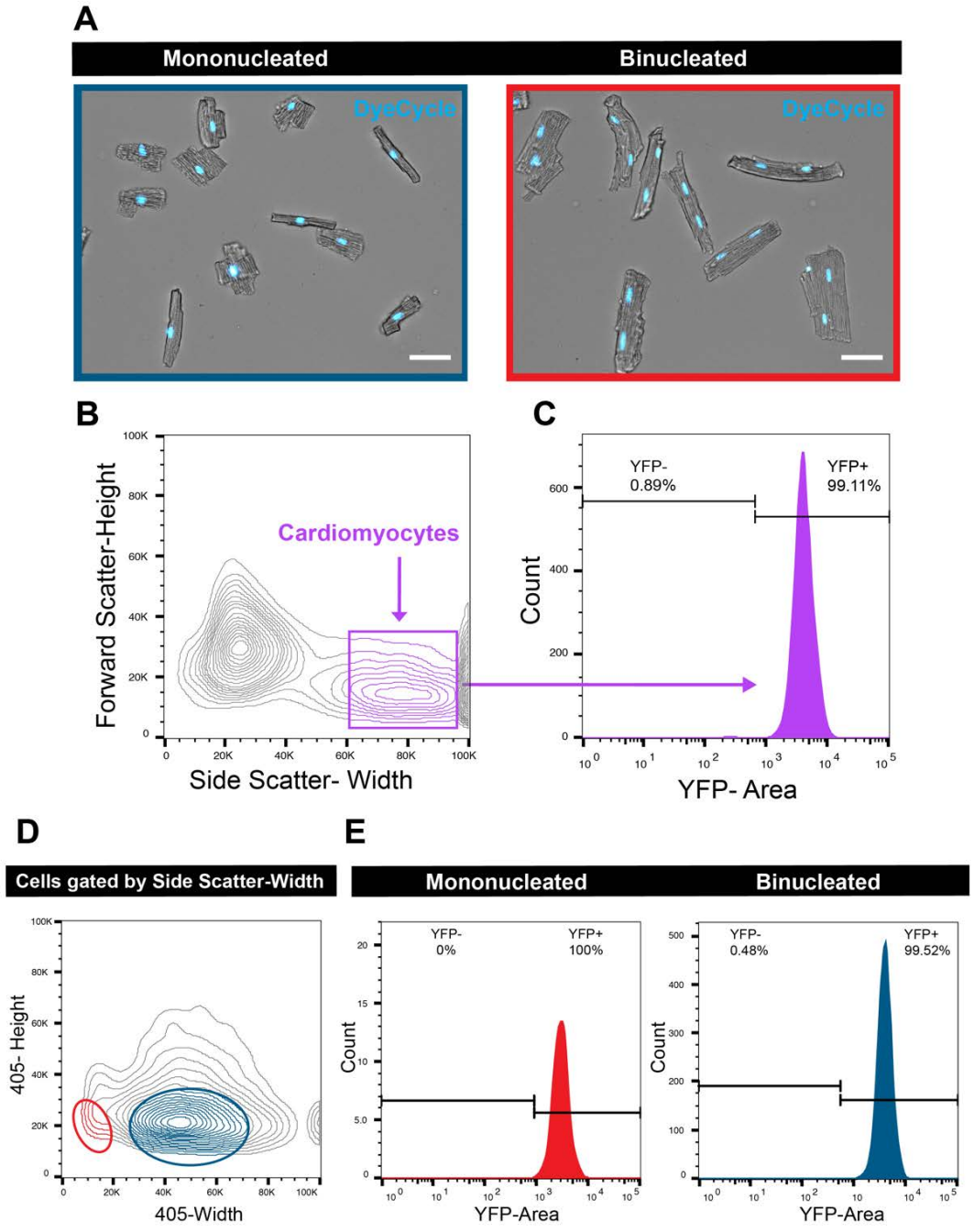

Figure 2.4 Expanded FACS strategy allows the sorting of cardiomyocytes without a lineage marker

(A) Adult CD-1 MoNuc and BiNuc cardiomyocytes sorted onto slides with expanded FACS strategy**.** Scale bar, 50 μm **(B)** FACS plots showing expanded FACS strategy. **(C)** The success of the expanded FACS strategy tested on Mlc2v^{cre}:R26R^{EYFP} cardiomyocytes. Histogram showing >99% of cells gated as cardiomyocytes are YFP+. **(D)** Testing relative ability of expanded FACS strategy to identify MoNucs and BiNucs as cardiomyocytes. FACS plot showing further gating of the cardiomyocytes identified in **(B)** to separate MoNucs and BiNucs. **(E)** Histograms showing lineage tracing of identified MoNucs and BiNucs. >99% of both MoNucs and BiNucs identified as cardiomyocytes by their light-scattering properties were YFP positive.

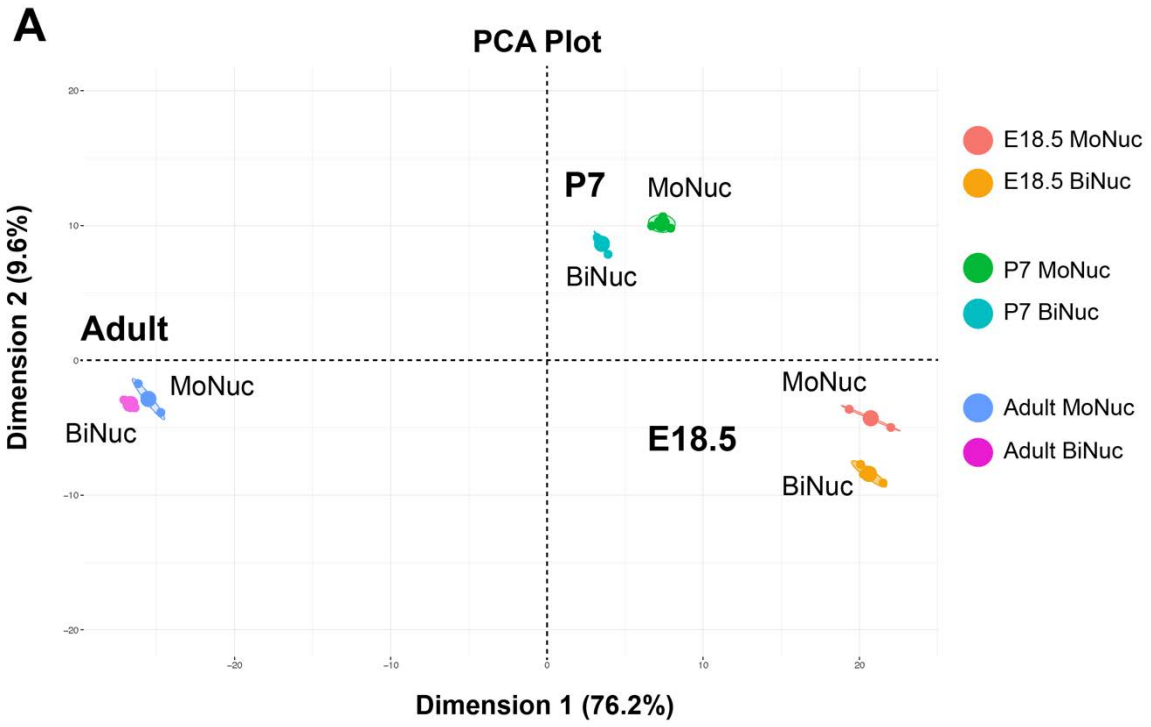

Figure 2.5 MoNucs and BiNucs are transcriptionally distinct at all analyzed timepoints

(A) Principal component analysis (PCA) from RNA-seq of MoNucs and BiNucs from E18.5, P7, and adult hearts shows that at each timepoint, MoNucs and BiNucs are transcriptionally distinct. n=3 animals per timepoint

Figure 2.6 RNA seq analysis of E18.5 MoNucs versus BiNucs

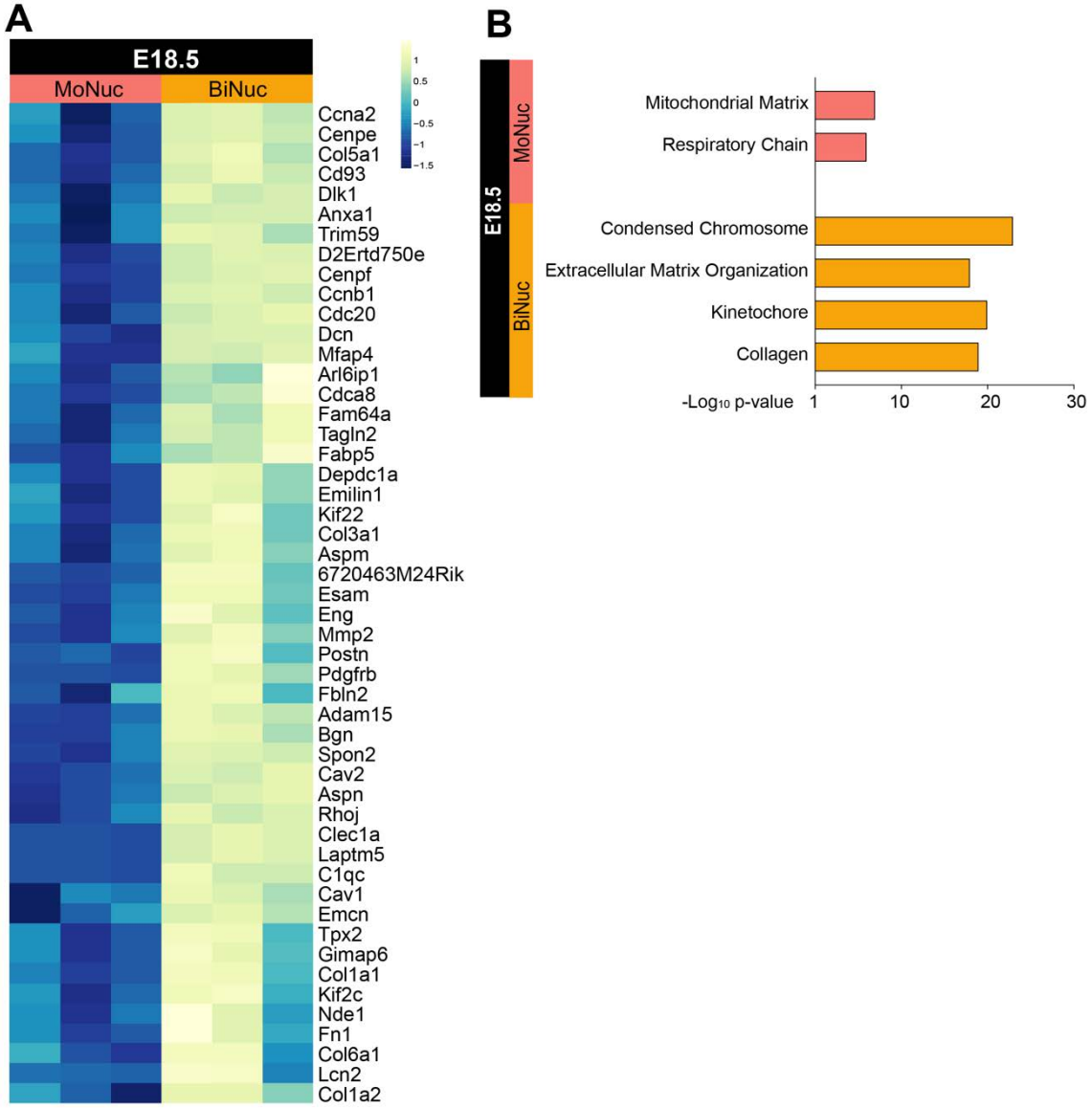

Figure 2.6 RNA seq analysis of E18.5 MoNucs versus BiNucs

(A) Heatmap of top 50 differentially expressed genes in E18.5 MoNucs versus BiNucs. **(B)** Representative categories from gene set enrichment analysis (GSEA) of differential gene expression between E18.5 MoNucs and BiNucs. Analysis was done using Camera. Results suggest that at E18.5, cardiomyocytes collected as BiNucs are likely still in the process of cytokinesis.

Figure 2.7 At P7, binucleation is accompanied by a switch from a proliferation-associated gene expression program to one associated with maturation

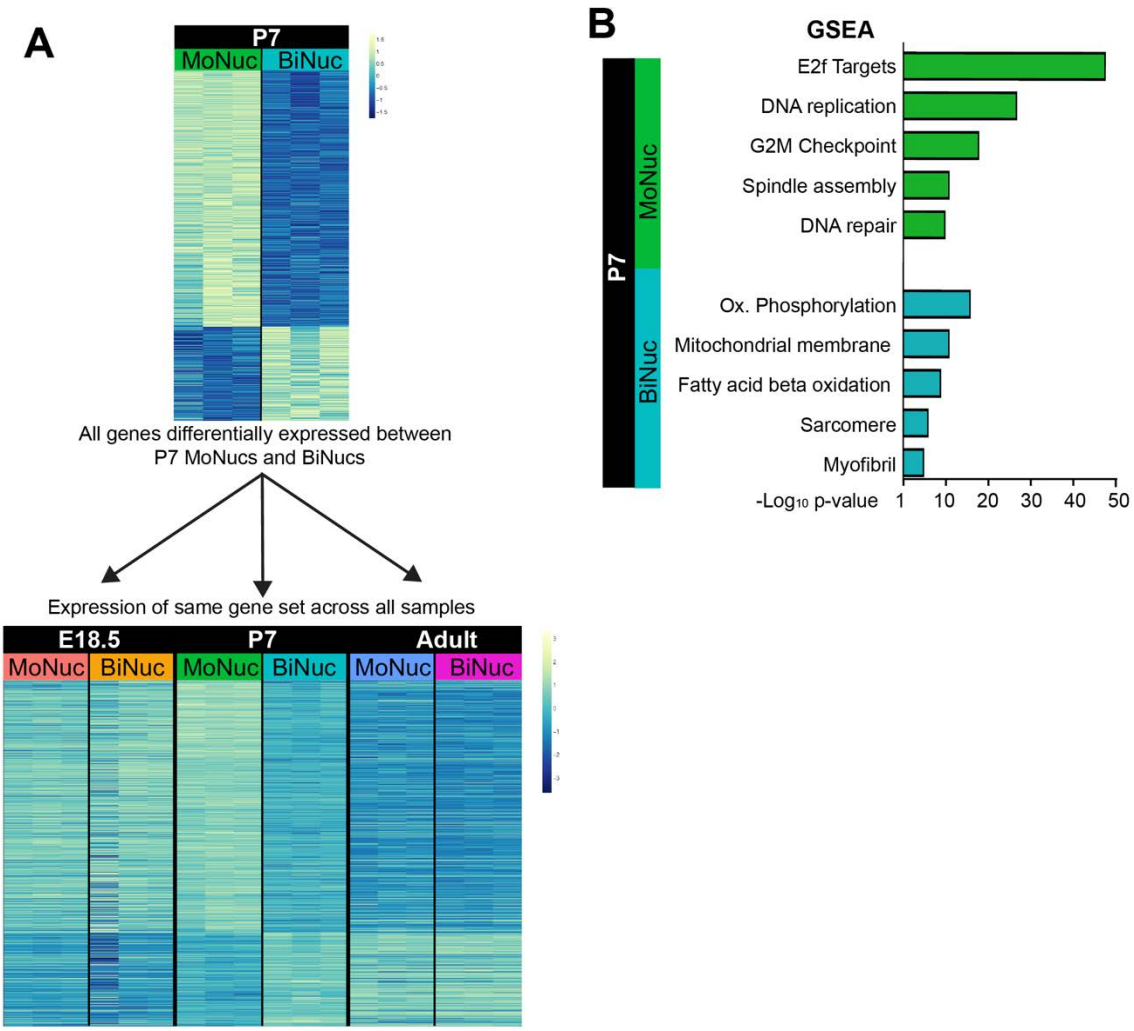

Figure 2.7 At P7, binucleation is accompanied by a switch from a proliferation-associated gene expression program to one associated with maturation

(A) Heatmaps of genes with significant differences (FDR < 0.05) in expression between P7 MoNucs and BiNucs. Gene expression values are represented at P7 only (top) and at all timepoints (bottom). The bottom heatmap reveals that the gene expression profile of P7 BiNucs but not P7 MoNucs shows resemblance to profiles of adult samples. The difference in intensity between the top and bottom heatmaps is due to the different scales used. **(B)** Representative categories from gene set enrichment analysis (GSEA) of differential gene expression between P7 MoNucs and BiNucs. P7 MoNucs are enriched for genes involved in the cell cycle, while P7 BiNucs are enriched for genes involved in cardiomyocyte maturation. Analysis was done using Camera.

Figure 2.8 Heatmaps of genes included in GSEA categories

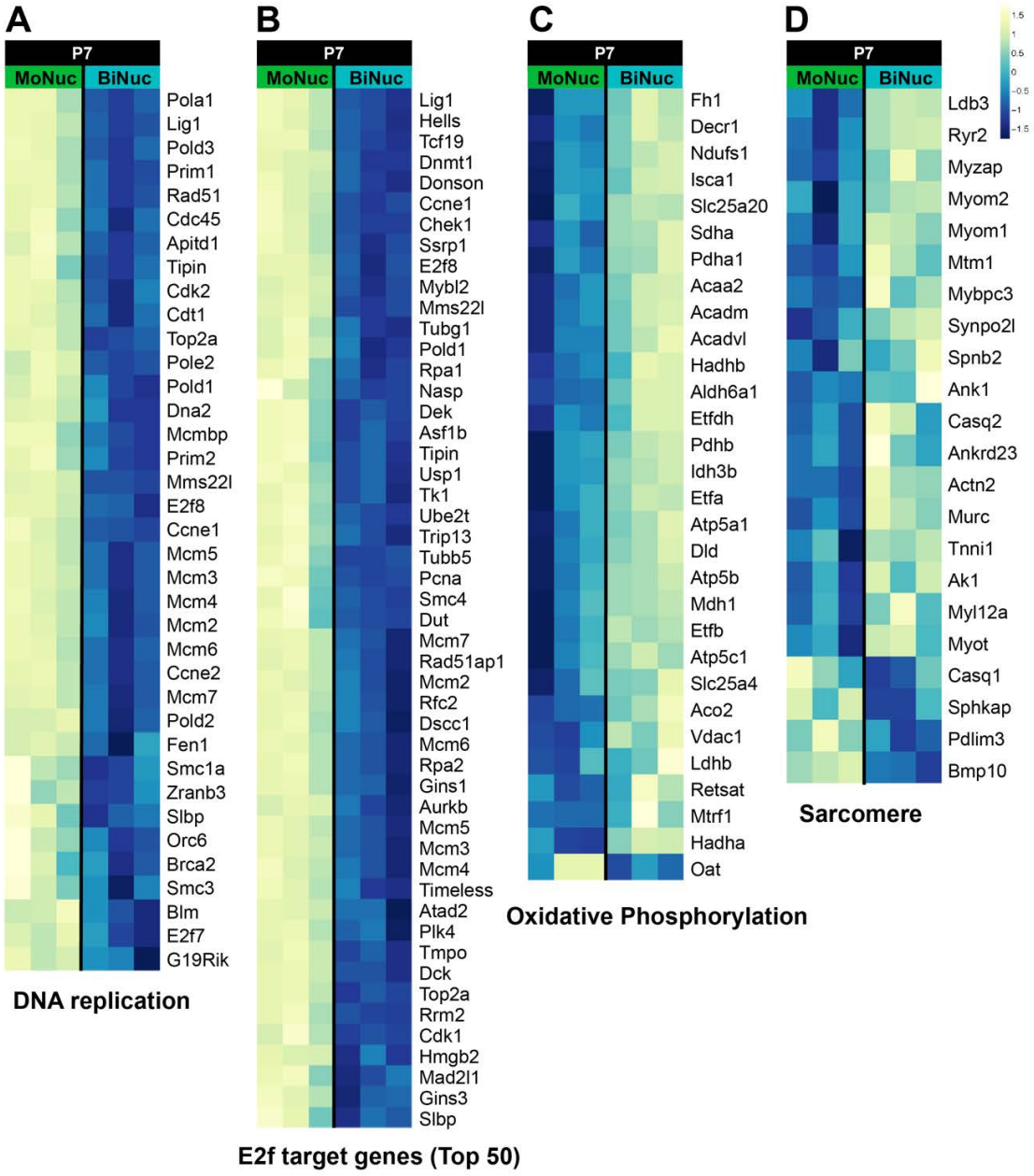

Figure 2.8 Heatmaps of genes included in GSEA categories

(A-D) Heatmaps of gene sets included in Figure 2.7. E2f target gene heatmap shows the top 50 differentially expressed genes from the set of 199 genes.

Figure 2.9 Binucleated cardiomyocytes at P7 turn off E2f target gene expression required for the G1/S phase transition and S phase

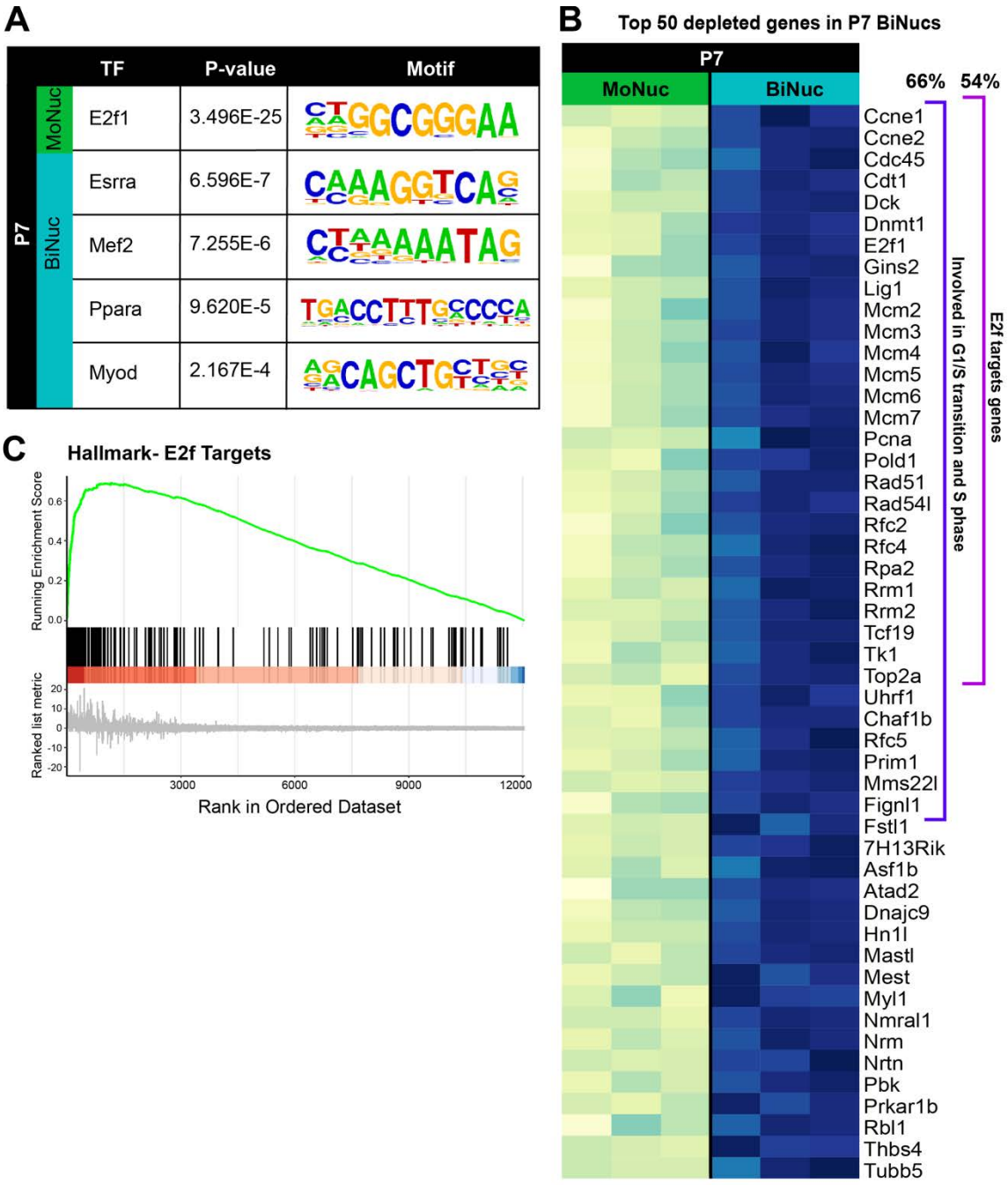

Figure 2.9 Binucleated cardiomyocytes at P7 turn off E2f target gene expression required for G1/S phase transition and S phase

(A) Enriched transcription factor motifs within promoters of genes differentially expressed between P7 MoNucs and BiNucs reveals E2f target genes are most highly enriched. Analysis was performed using the Toppgene suite. **(B)** Analysis of the top 50 differentially expressed genes between P7 MoNucs and BiNucs reveals 66% (33/50) are involved in G1/S transition and S phase of the cell cycle, 27 of which (54%, 27/50) are E2f target genes. **(C)** Gene set enrichment analysis plot of E2f target genes differentially expressed between P7 MoNucs and BiNucs.

Figure 2.10 E2f target gene expression decreases specifically between P7 MoNucs and BiNucs

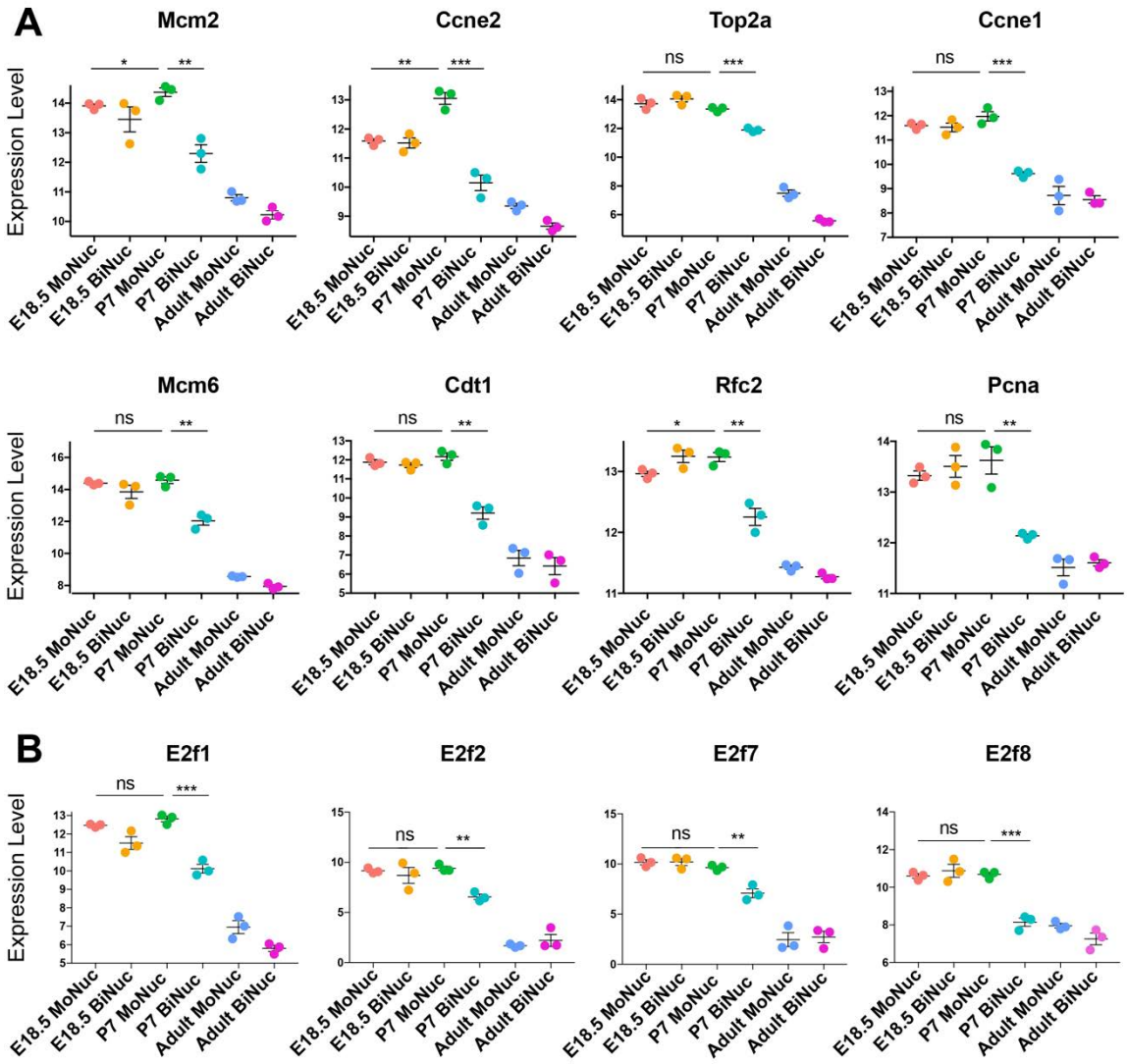

Figure 2.10 E2f target gene expression decreases specifically between P7 MoNucs and BiNucs

Expression values of **(A)** E2f target genes and **(B)** indicated E2f family members and are shown across all samples. Significance of differences in gene expression between E18.5 and P7 MoNucs and between P7 MoNucs and BiNucs are indicated. Data are mean ± SEM. n=3 animals per timepoint. p-values are determined by student's t-test. ns=not significant, *=p<0.05, **=p<0.01, ***=p<0.001, ****=p<0.0001.

Figure 2.11 Adult mononucleated and binucleated cardiomyocytes retain differences established during neonatal maturation

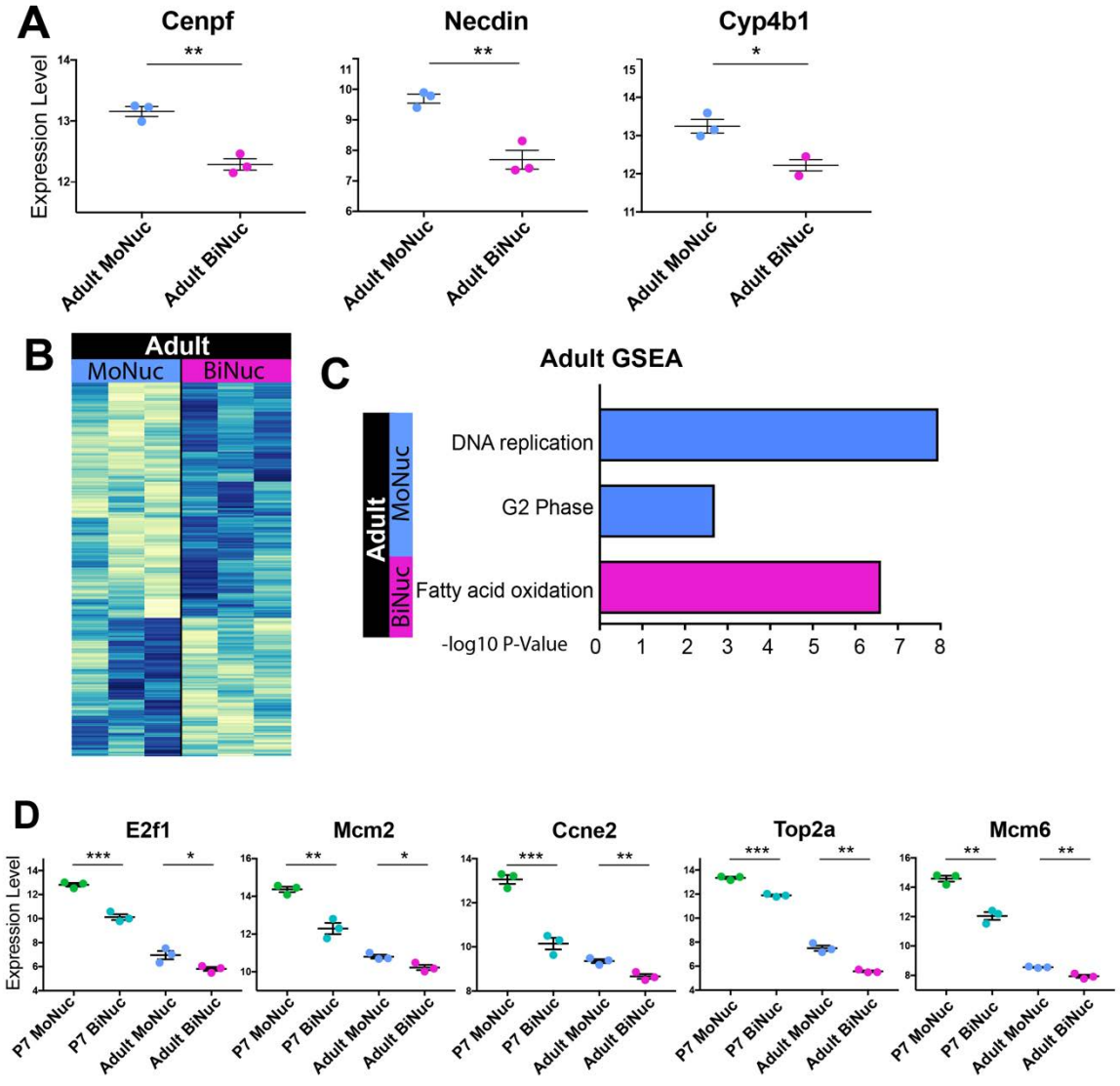

Figure 2.11 Adult mononucleated and binucleated cardiomyocytes retain differences established during neonatal maturation

(A) Expression values measured by RNA-seq of genes with FDR < 0.05 between adult MoNucs and BiNucs. Data are mean ± SEM. n=3 animals per timepoint. **(B)** Heatmap of gene expression differences with p-value < 0.05 between Adult MoNucs and BiNucs. **(C)** Representative categories from gene set enrichment analysis (GSEA) of differential gene expression between Adult MoNucs and BiNucs reveals overlap with categories enriched between P7 MoNucs and BiNucs. Analysis was done using Camera. **(D)** A subset of E2f target genes most differentially expressed between P7 MoNucs and BiNucs remain differentially expressed between Adult MoNucs and BiNucs. The expression values of these genes are shown in P7 and Adult samples. Significance of differences in gene expression between P7 MoNucs and BiNucs and between Adult MoNucs and BiNucs are indicated. Data are mean ± SEM. n=3 animals per timepoint. p-values are determined by student's t-test. ns=not significant, *=p<0.05, **=p<0.01, ***=p<0.001, ****=p<0.0001.

Figure 2.12 Adult BiNucs have a higher density of glycogen granules

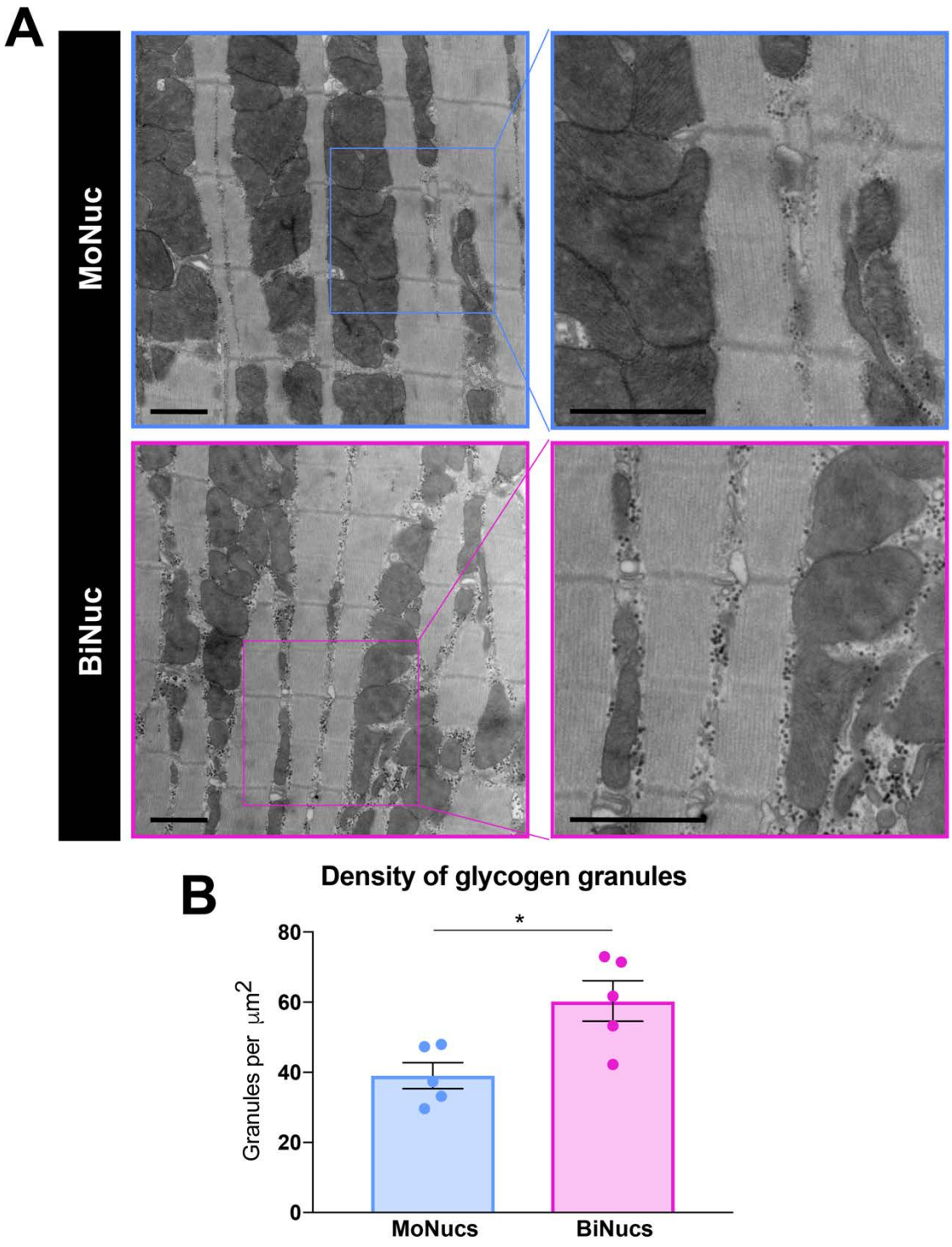

Figure 2.12 Adult BiNucs have a higher density of glycogen granules.

(A) Electron micrographs of sorted adult MoNucs and BiNucs. Scale bar, 1 μm. **(B)** Quantification of glycogen granule density in non-sarcomeric cytoplasmic space visualized by electron microscopy. Significance of difference between adult MoNucs and BiNucs is indicated Data are mean ± SEM. n=5 cells per sample. p-values are determined by student's t-test. ns=not significant, *=p<0.05, **=p<0.01, ***=p<0.001, ****=p<0.0001.

Figure 2.13 Rb acts downstream of binucleation and is required for downregulation of E2f target genes

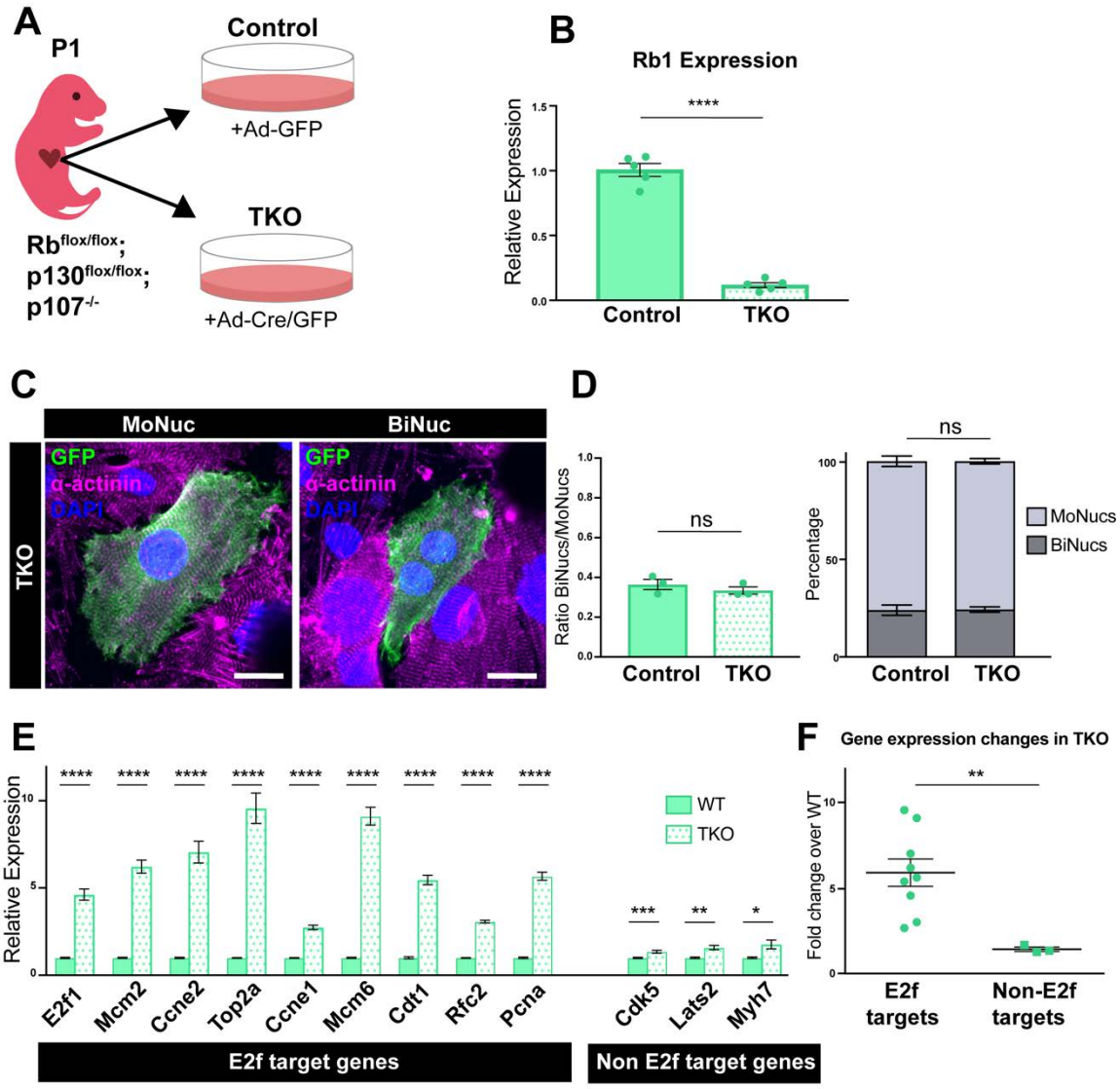

Figure 2.13 Rb acts downstream of binucleation and is required for downregulation of E2f target genes

(A) Schematic of experimental design of *in vitro* Rb family knockout experiments. Cardiomyocytes were isolated from $Rb^{flox/flox}$;$p130^{flox/flox}$;$p107^{-/-}$ mice at P1 and infected with adenovirus containing either Cre and GFP (Ad-Cre/GFP) or GFP alone (Ad-GFP). Cells infected with Ad-Cre/GFP are denoted as Triple Knockout (TKO) samples, and cells infected with Ad-GFP are denoted as Control samples. **(B)** Expression values of the Rb transcript in TKO samples compared to control samples by qPCR. Data are mean ± SEM. n=5 animals. **(C)** Confocal images of fixed TKO MoNuc and BiNuc cardiomyocytes stained with antibodies against α-actinin and GFP. Scale bar, 20 μm. **(D)** Quantification of the ratio of BiNucs to MoNucs and percentages of MoNucs and BiNucs in GFP+ control and TKO cardiomyocytes fixed and stained with antibodies against α-actinin and GFP. n=3 animals. Data are mean ± SEM. p-values are determined by student's t-test **(E)** Gene expression differences between Control and TKO samples of E2f target genes and non-E2f target genes by qPCR. Data are mean ± SEM. n=5 animals. p-values are determined by student's t-test. **(F)** Comparison of mean fold change expression of TKO samples over control samples of E2f target genes versus non-E2f target genes. p-values are determined by student's t-test. ns=not significant, *=$p<0.05$, **=$p<0.01$, ***=$p<0.001$, ****=$p<0.0001$.

Table 2.1 Top 10 upregulated Gene Ontology and Hallmark categories at P7 (Enriched in MoNucs at P7)

GO Category	Direction	PValue	FDR
GO:0006261 DNA-dependent DNA replication	Up	2.18E-27	3.27E-23
GO:0005657 replication fork	Up	4.05E-26	3.03E-22
GO:0006270 DNA replication initiation	Up	6.45E-26	3.22E-22
GO:0006260 DNA replication	Up	2.02E-23	7.56E-20
GO:0042555 MCM complex	Up	3.99E-17	1.19E-13
GO:0030894 replisome	Up	2.48E-15	6.20E-12
GO:0007059 chromosome segregation	Up	4.44E-15	9.50E-12
GO:0000793 condensed chromosome	Up	7.72E-15	1.45E-11
GO:0043596 nuclear replication fork	Up	4.88E-14	8.13E-11
GO:0000775 chromosome, centromeric region	Up	6.55E-14	9.82E-11
Hallmark Category	**Direction**	**PValue**	**FDR**
HALLMARK_E2f_targets	Up	1.44E-48	7.19E-47
HALLMARK_G2M_checkpoint	Up	8.14E-18	2.03E-16
HALLMARK_epithelial_mesenchymal_transition	Up	2.18565E-05	0.000182137
HALLMARK_DNA_repair	Up	0.001340747	0.009576765
HALLMARK_cholesterol_homeostasis	Up	0.004767588	0.026879478
HALLMARK_estrogen_response_late	Up	0.004838306	0.026879478
HALLMARK_Myc_targets_V1	Up	0.007929791	0.039648953
HALLMARK_mitotic_spindle	Up	0.013387727	0.060853302
HALLMARK_UV_response_up	Up	0.041094641	0.139505466
HALLMARK_apical_junction	Up	0.052624342	0.154777475

Table 2.2 Top 10 downregulated Gene Ontology and Hallmark categories at P7 (Enriched in BiNucs at P7)

GO Category	Direction	PValue	FDR
GO:0044455 mitochondrial membrane part	Down	4.17E-11	3.47E-08
GO:0006099 tricarboxylic acid cycle	Down	5.58E-11	4.40E-08
GO:0070469 respiratory chain	Down	6.97E-11	5.22E-08
GO:0005746 mitochondrial respiratory chain	Down	4.76E-10	2.55E-07
GO:0045333 cellular respiration	Down	1.40E-09	5.39E-07
GO:0005743 mitochondrial inner membrane	Down	1.88E-09	6.71E-07
GO:0006635 fatty acid beta-oxidation	Down	6.45E-09	2.10029E-06
GO:0005747 mitochondrial respiratory chain complex I	Down	1.93E-08	5.35634E-06
GO:0030964 NADH dehydrogenase complex	Down	1.93E-08	5.35634E-06
GO:0045271 respiratory chain complex I	Down	1.93E-08	5.35634E-06
Hallmark Category	**Direction**	**PValue**	**FDR**
HALLMARK_oxidative_phosphorylation	Down	2.67E-16	4.44E-15
HALLMARK_adipogenesis	Down	8.34E-07	1.04207E-05
HALLMARK_fatty_acid_metabolism	Down	6.47395E-06	6.47395E-05
HALLMARK_bile_acid_metabolism	Down	0.014783457	0.061597739
HALLMARK_protein_secretion	Down	0.030395013	0.116903895
HALLMARK_peroxisome	Down	0.04207603	0.139505466
HALLMARK_heme_metabolism	Down	0.044641749	0.139505466
HALLMARK_myogenesis	Down	0.100500333	0.228409848
HALLMARK_notch_signaling	Down	0.227691276	0.44370498
HALLMARK_p53_pathway	Down	0.239600689	0.44370498

Table 2.3 All differentially expressed Gene Ontology and Hallmark categories in Adult MoNucs versus BiNucs

GO Category	Direction	PValue	FDR
GO:0000085 G2 phase of mitotic cell cycle	Up	9.08E-08	0.000680188
GO:0051319 G2 phase	Up	9.08E-08	0.000680188
GO:0072329 monocarboxylic acid catabolic process	Down	3.98E-07	0.001050164
GO:0009062 fatty acid catabolic process	Down	4.54E-07	0.001050164
GO:0019395 fatty acid oxidation	Down	5.87E-07	0.001050164
GO:0034440 lipid oxidation	Down	5.87E-07	0.001050164
GO:0018879 biphenyl metabolic process	Up	6.31E-07	0.001050164
GO:0018917 fluorene metabolic process	Up	6.31E-07	0.001050164
GO:0018585 fluorene oxygenase activity	Up	6.31E-07	0.001050164
GO:0006635 fatty acid beta-oxidation	Down	1.50631E-06	0.002256606
GO:0070402 NADPH binding	Down	1.22356E-05	0.015973572
GO:0030258 lipid modification	Down	1.27951E-05	0.015973572
GO:0006733 oxidoreduction coenzyme metabolic process	Down	3.13271E-05	0.036100915
GO:0003995 acyl-CoA dehydrogenase activity	Down	4.24762E-05	0.045452598
HALLMARK Category	**Direction**	**PValue**	**FDR**
HALLMARK_fatty_acid_ metabolism	Down	2.16142E-05	0.001080708
HALLMARK_adipogenesis	Down	0.000156879	0.003921965
HALLMARK_epithelial_mesenchymal_transition	Up	0.002099963	0.028172254
HALLMARK_oxidative_ phosphorylation	Down	0.00225378	0.028172254
HALLMARK_bile_acid_ metabolism	Down	0.00377872	0.037787197

CHAPTER 3: BINUCLEATION LEADS TO SILENCING OF E2F TRANSCRIPTION FACTOR ACTIVITY AND IMPAIRS REGENERATIVE CAPACITY DURING THE NEONATAL PERIOD

3.1 SUMMARY

The data presented in Chapter 2 showed that down-regulation of E2f target genes, a process that requires Rb, occurs in BiNucs at P7 but is not responsible for inducing binucleation. In Chapter 3, we examine whether these transcriptional changes instead occur as a result of binucleation. We utilized a genetic mouse model to alter the ratio of BiNucs to MoNucs during the neonatal maturation period to establish a direct link between binucleation and E2f signaling. We also used this genetic model to examine the relationship between binucleation and loss of regenerative ability in the heart.

3.2 INTRODUCTION

During cytokinesis, the contractile ring is formed beneath the plasma membrane around the equator of the mitotic cell (Tucker, 1971). It is built by regulatory proteins at the initiation of cytokinesis, and its constriction carries the plasma membrane with it towards the cell's center, thus dividing the cell in half. Over a range of cell types and organisms, the RhoA GTPase pathway is responsible for orchestrating the formation and contraction of the contractile ring during cytokinesis (Kamijo et al., 2006). Ect2 is the guanine nucleotide exchange factor (GEF) responsible for activating RhoA and is

required for successful cytokinesis (Fields and Justilien, 2010; Tatsumoto et al., 1999) (Figure 3.1). We hypothesized that loss of Ect2 in cardiomyocytes would result in failed cytokinesis and, therefore, an increase in the proportion of binucleated cardiomyocytes in the heart during the neonatal period. This model would allow us to draw direct links between binucleation and its downstream effects.

3.3 LOSS OF ECT2 IN EMBRYONIC CARDIOMYOCYTES RESULTS IN INCREASED CARDIOMYOCYTE BINUCLEATION AND IS LETHAL

We generated an $Ect2^{flox/flox}$ allele and first crossed it with the cardiomyocyte-specific $Nkx2.5^{cre}$ allele. $Nkx2.5^{cre}$:$Ect2^{flox/flox}$ mice did not survive beyond E10.5 (Figure 3.2A, C, D). At E10.5 $Nkx2.5^{cre}$:$Ect2^{flox/flox}$ mice had altered myocardial morphology and a significant decrease in ventricular Ect2 expression (Figure 3.2B-D). E10.5 $Nkx2.5^{cre}$:$Ect2^{flox/flox}$ mutant hearts were primarily comprised of BiNucs, while control hearts were comprised almost exclusively of MoNucs. The mean ratio of BiNucs to MoNucs increased from 0.026 ± 0.01 in control hearts to 3.716 ± 0.07 in mutant hearts. (Figure 3.2E-F).

3.4 BINUCLEATION RESULTS IN SILENCING OF E2F TRANSCRIPTIONAL TARGETS

Next, we crossed our $Ect2^{flox/flox}$ allele with the $Mlc2v^{cre}$ allele. Mlc2vcre shows cardiomyocyte-specific expression in a mosaic fashion (Gillers et al., 2015; Guimaraes-Camboa et al., 2015). We harvested knockout and control hearts at an early and late neonatal timepoint. At P7, there was no difference in Ect2 expression levels between $Mlc2v^{cre}$:$R26R^{EYFP}$ and control hearts (Figure 3.3A-B). This is likely because Ect2 expression decreases over the neonatal period, so baseline Ect2 levels would be too low to observe a difference between the control and knockout animals. Similarly, there was no difference in the ratio of BiNucs to MoNucs or in the relative expression of E2f target genes between $Mlc2v^{cre}$:$R26R^{EYFP}$ and control mice at P7 (Figure 3.3C-D). In $Mlc2v^{cre}$:$R26R^{EYFP}$ hearts, we saw an increase in the proportion of cells expressing YFP between E18.5 and P2 by FACS, suggesting that cre-mediated recombination increases during the early neonatal period (Figure 3.4). Therefore, we next examined $Mlc2v^{cre}$:$Ect2^{flox/flox}$ mutants at P3, at which time they exhibited a 61.8% decrease in Ect2 expression compared to controls (Figure 3.5A-B). $Mlc2v^{cre}$:$Ect2^{flox/flox}$ mutants had an increase in the mean ratio of BiNucs to MoNucs at P3 of 0.901 ± 0.08 compared to 0.339 ± 0.02 in control mice (Figure 3.5C-D). QPCR revealed a significant decrease in expression of E2f target genes in $Mlc2v^{cre}$:$Ect2^{flox/flox}$ mutants compared to controls but no significant change in genes that are not E2f targets (Figure 3.5E-F). These data

suggest that the downregulation of E2f target genes occurs as a direct result of binucleation in cardiomyocytes.

3.5 BINUCLEATION IMPAIRS REGENERATIVE ABILITY

To examine whether these events impair the regenerative ability of the heart, we performed LAD ligation to induce myocardial infarction in $Mlc2v^{cre}$:$Ect2^{flox/flox}$ mutants and control mice at P1 (Figure 3.6A). At this developmental timepoint, the murine heart is still able to mount a substantial regenerative response to injury (Porrello et al., 2011). We observed that at P8, a higher percentage of myocardium remained as scar tissue in $Mlc2v^{cre}$:$Ect2^{flox/flox}$ mutants compared to control mice. (Figure 3.6B-C). This data supports a model whereby binucleation directly results in decreased competency for proliferation and regeneration via an Rb/E2f pathway.

3.1 The critical role of Ect2 in cytokinesis

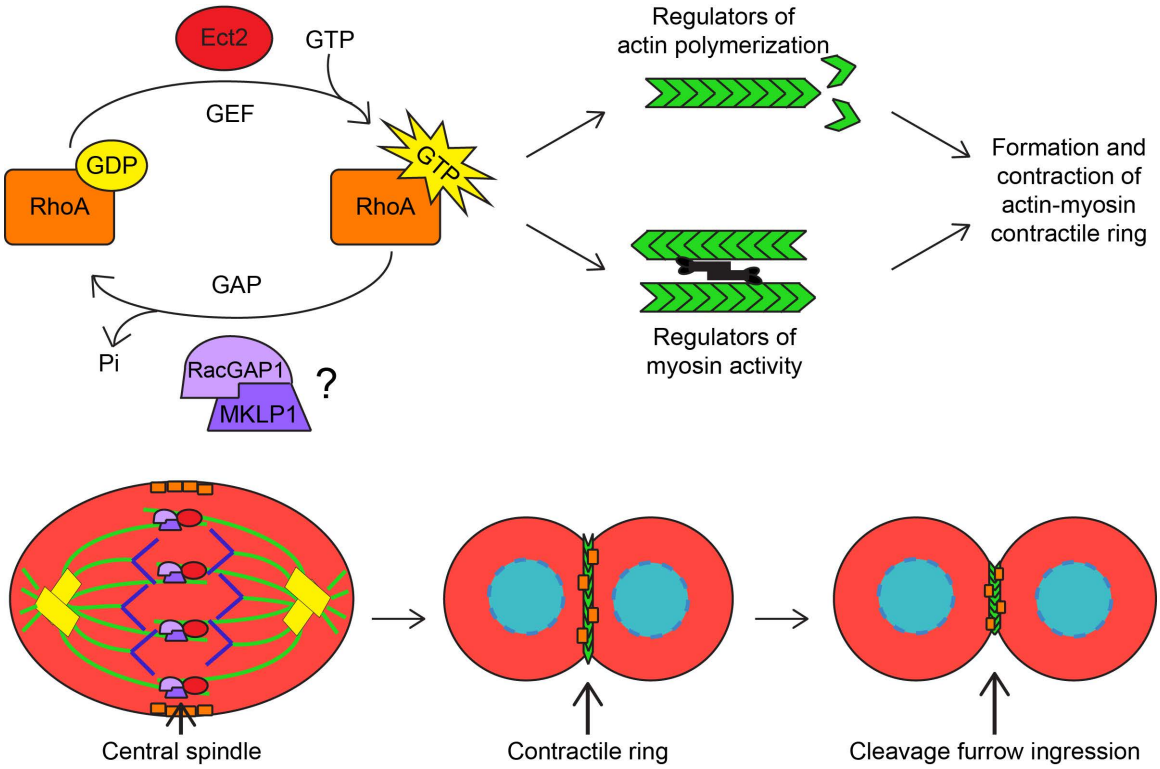

3.1 The critical role of Ect2 in cytokinesis

Ect2 acts as the Guanine nucleotide exchange factor (GEF) for the RhoA GTPase. RacGap1 may act as the GTPase activating protein (GAP) for RhoA. RacGap and MKLP1 form the centralspindlin complex, which recruits Ect2 to the central spindle. The interaction between centralspindlin and Ect2 is required for Ect2 to be active, which allows for the location of Ect2 activity to be tightly regulated. Active Ect2 activates RhoA in a locally precise manner in the overlying cortex by exchanging GDP for GTP. Active RhoA is responsible for inducing actin polymerization and activating myosin to form the contractile ring. RhoA is also responsible for regulating the actions of several additional proteins that induce the contraction of the contractile ring leading to cleavage furrow formation and ingression.

Figure 3.2 Loss of Ect2 in the embryonic heart results in binucleation of cardiomyocytes and is lethal

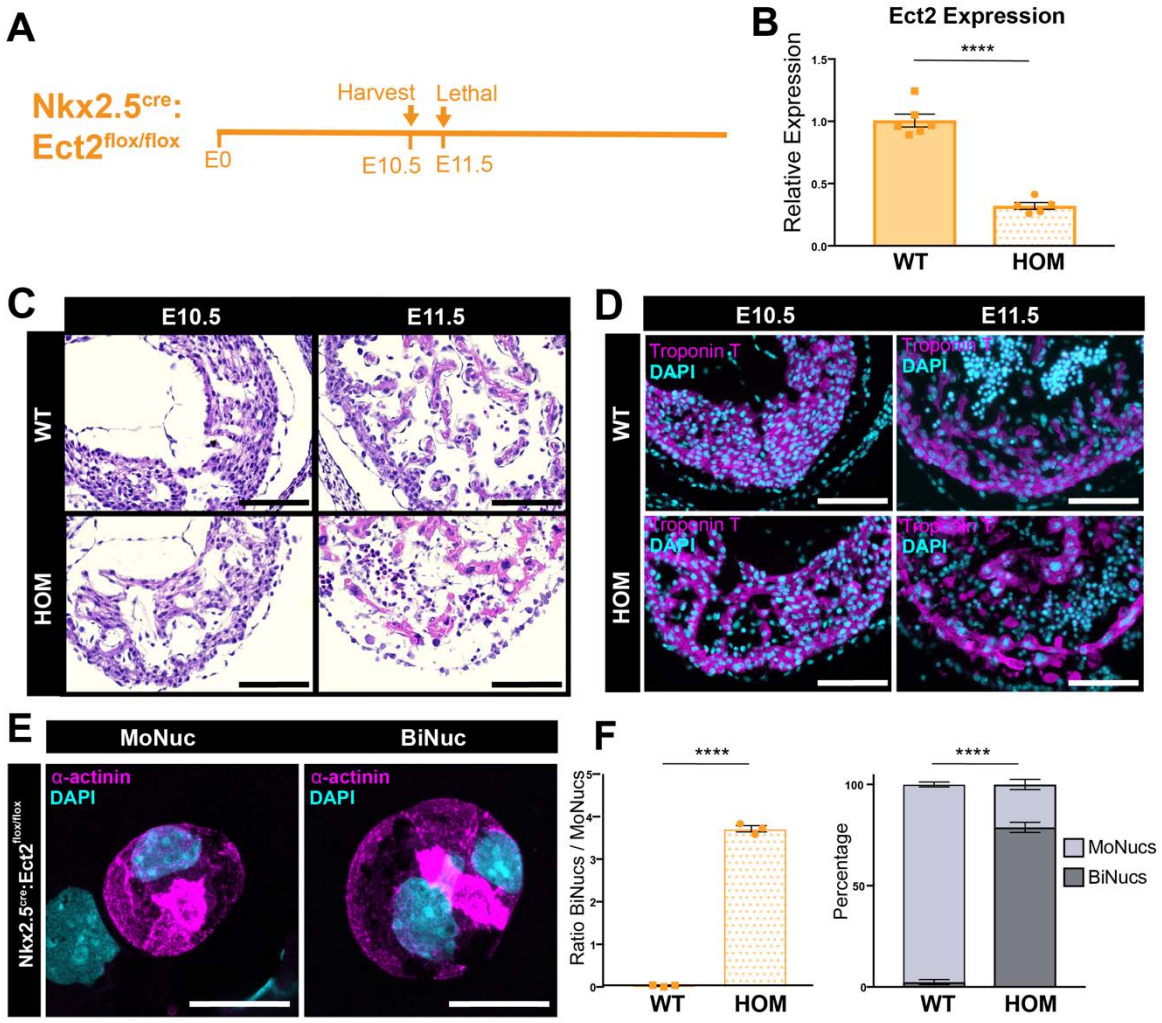

Figure 3.2 Loss of Ect2 in the embryonic heart results in binucleation of cardiomyocytes and is lethal

(A) Timecourse of Ect2 knockout using Nkx2.5^{cre}. **(B)** Expression values of the Ect2 transcript in Nkx2.5^{cre}:Ect2$^{flox/flox}$ (HOM) samples compared to Ect2$^{flox/flox}$ and Ect2$^{flox/+}$ (WT) samples at E10.5 by qPCR. Data are mean ± SEM. n=5-6 animals per group **(C-D)**. Representative tissue sections of WT and HOM hearts at E10.5 and E11.5 stained with H&E **(C)** or an antibody against cardiac Troponin T **(D)** reveals that the Nkx2.5^{cre}:Ect2$^{flox/flox}$ allele is lethal by E11.5. Scale bar, 100 μm. **(D)** Representative images of a MoNuc and BiNuc present in E10.5 HOM samples. Single-cell suspensions were cytospun and stained with an antibody against α-actinin. Scale bar, 20 μm. **(E)** Quantification of the ratio of BiNucs to MoNucs and percentages of MoNucs and BiNucs in E10.5 WT and HOM samples. Data are mean ± SEM. n=3 animals per group. p-values are determined by student's t-test. ns=not significant, *=p<0.05, **=p<0.01, ***=p<0.001, ****=p<0.0001.

Figure 3.3 By P7, no differences are observed between Mlc2v^{cre}:Ect2$^{flox/flox}$ and control mice

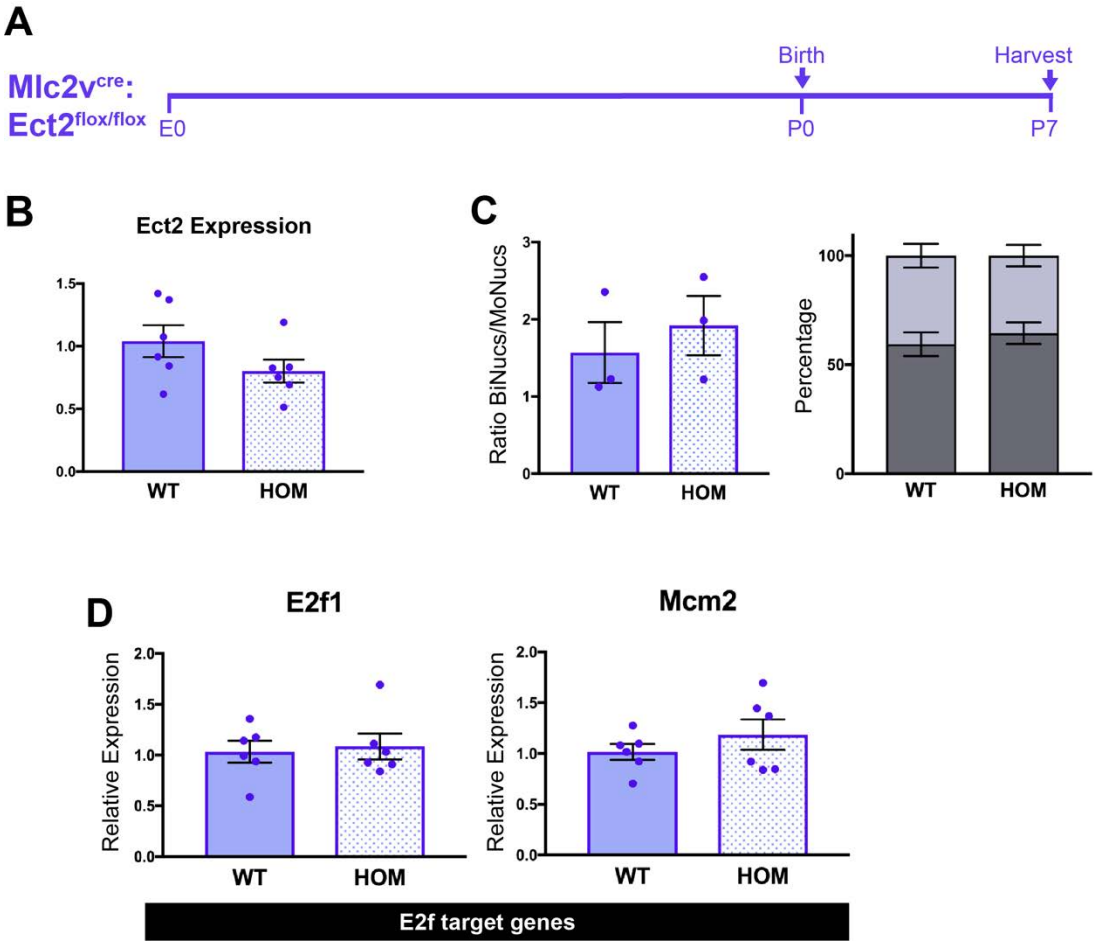

Figure 3.3 By P7, no differences are observed between Mlc2v^{cre}:Ect2$^{flox/flox}$ and control mice

(A) Timecourse of the first set of experiments knocking out Ect2 with Mlc2v^{cre}. **(B)** Expression values of the Ect2 transcript in Mlc2v^{cre}:Ect2$^{flox/flox}$ (HOM) samples compared to Ect2$^{flox/flox}$ and Ect2$^{flox/+}$ (WT) samples at P7 by qPCR. Data are mean ± SEM. n=6 animals per group. **(C)** Quantification of the ratio of BiNucs to MoNucs and percentages of MoNucs and BiNucs in P7 WT and HOM samples. Quantification of MoNucs and BiNucs was done by FACS. Data are mean ± SEM. n=3 animals per group. **(D)** Gene expression differences between WT and HOM samples of E2f target genes at P7. Data are mean ± SEM. n=6 animals per group. p-values are determined by student's t-test. ns=not significant.

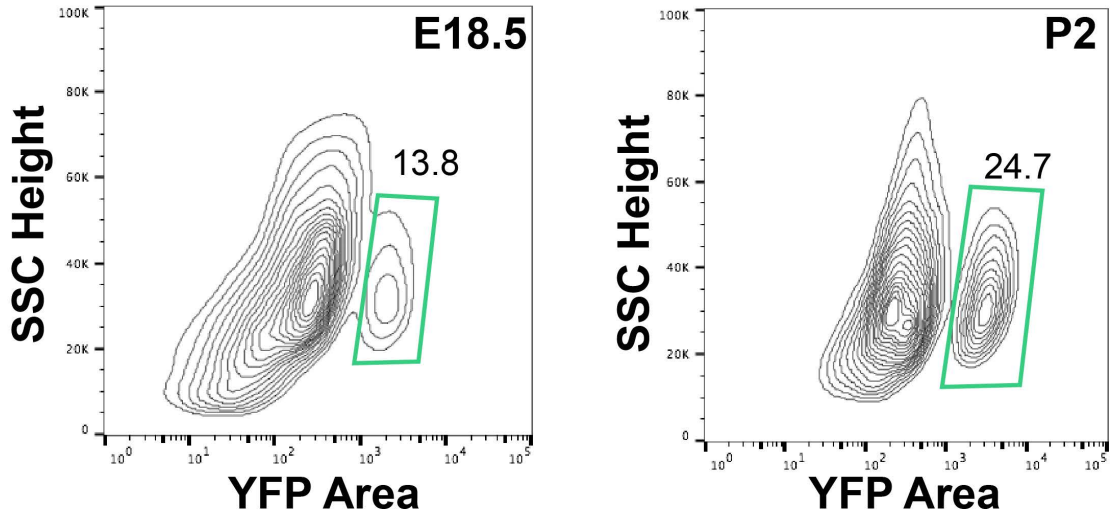

Figure 3.4 Mlc2v^{cre} recombination increases during the early neonatal period

FACS plots of YFP presence in cells from Mlc2v^{cre}:R26R^{EYFP} hearts at E18.5 and P2 show an increase in YFP+ cells between E18.5 and P2. This suggests that Mlc2v^{cre} recombination occurs in at least a subset of cardiomyocytes during the neonatal period.

Figure 3.5 Mlc2v^{cre}:Ect2$^{flox/flox}$ results in increased binucleation at postnatal day 3

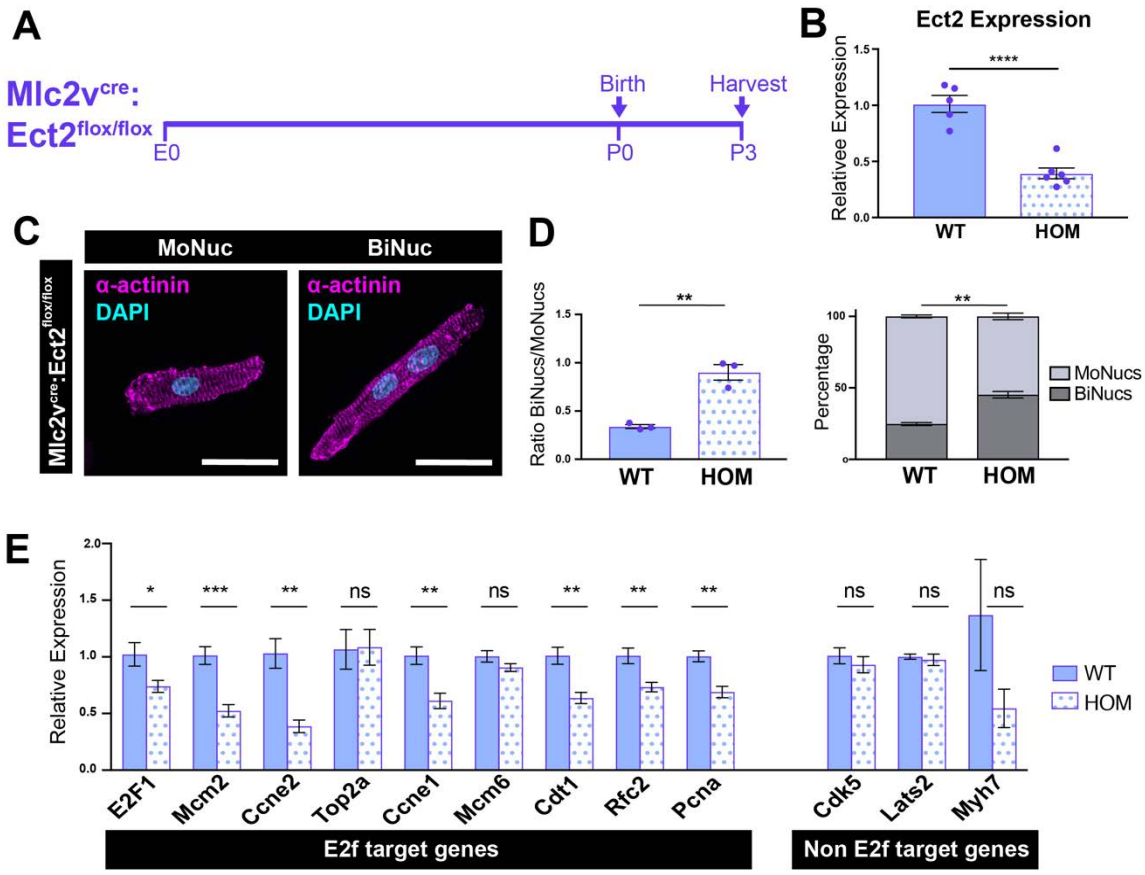

Figure 3.5 Mlc2v^{cre}:Ect2$^{flox/flox}$ results in increased binucleation at postnatal day 3

(A) Timecourse of the second set of Ect2 knockout experiments using Mlc2v^{cre}. **(B)** Expression values of the Ect2 transcript in Mlc2v^{cre}:Ect2$^{flox/flox}$ (HOM) samples compared to Ect2$^{flox/flox}$ and Ect2$^{flox/+}$ (WT) samples at P3 by qPCR. Data are mean ± SEM. n=5-6 animals per group. **(C)** Images of P3 HOM MoNuc and BiNuc cardiomyocytes from fixed single-cell suspensions stained with anti-α-actinin. Scale bar, 20 μm. **(D)** Quantification of the ratio of BiNucs to MoNucs and percentages of MoNucs and BiNucs in P3 WT and HOM samples. Data are mean ± SEM. n=3 animals per group. **(E)** Gene expression differences between WT and HOM samples of E2f target genes and non-E2f target genes. Data are mean ± SEM. n=5-6 animals per group. p-values are determined by student's t-test. ns=not significant, *=p<0.05, **=p<0.01, ***=p<0.001, ****=p<0.0001.

Figure 3.6 Neonatal binucleation impairs regenerative potential

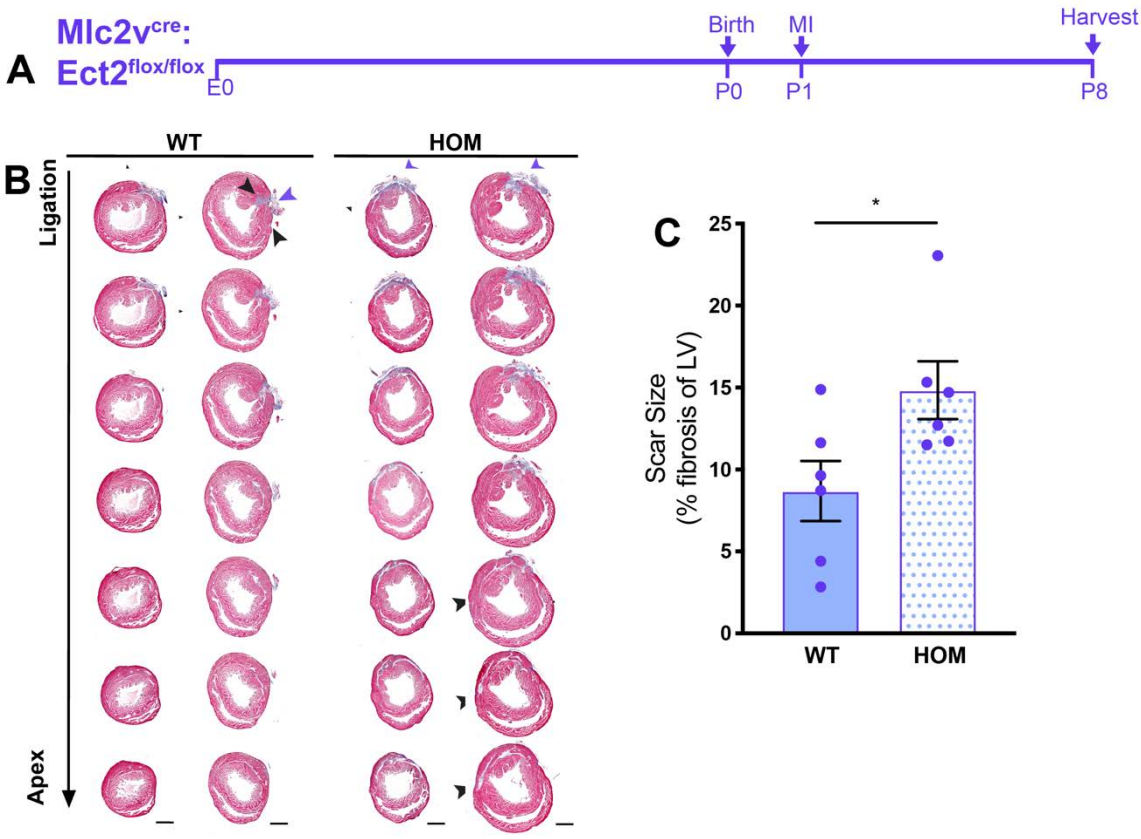

Figure 3.6 Binucleation impairs regenerative potential

(A) Schematic showing study design of MI by ligation of the left anterior descending (LAD) artery in Mlc2v^{cre}:Ect2$^{flox/flox}$ mutant and control mice at P1. **(B)** Masson's trichrome–stained heart sections from the ligation site toward the apex 7 days after injury. n=6 per group **(C)** Quantification of the percent of left ventricular myocardium containing scar tissue at P8. The suture location is indicated with a purple arrow. Scar boundaries are indicated with black arrows. Scale bar, 500 μm. Data are mean ± SEM. n=6 animals per group. p-values are determined by the Mann-Whitney U test. ns=not significant, *=p<0.05, **=p<0.01, ***=p<0.001, ****=p<0.0001.

CHAPTER 4: CONCLUSIONS AND FUTURE DIRECTIONS

4.1 DISCUSSION

A lack of effective therapeutic strategies to treat the acutely injured heart has led scientists to search for a means to replace cardiomyocytes that have been lost due to injury. One compelling approach would be to develop therapies that activate endogenous cardiomyocyte proliferation to regenerate damaged tissue. While previous work has suggested a correlation between cardiomyocyte nucleation and the ability to re-enter the cell cycle, with MoNucs being more receptive to proliferative stimuli, the molecular basis for this difference has remained elusive, likely due to the technical hurdles in isolating and independently characterizing MoNucs and BiNucs. To address this question, I developed a novel FACS-based strategy to isolate these two cardiomyocyte populations at embryonic, neonatal, and adult timepoints. This methodological advancement allowed us to carry out the first characterization of the molecular differences between MoNucs and BiNucs. It will also allow for continued future work toward better understanding the differences between these two cardiomyocyte subsets. Furthermore, I expanded this FACS based approach to sort total adult cardiomyocytes without the use of a lineage label. This strategy takes advantage of the large size and unique shape of cardiomyocytes to separate them from the other cell types in the heart based on the same principles underlying the separation of MoNucs from BiNucs.

The MoNuc and BiNuc cardiomyocyte subsets diverge during a neonatal period during which time cardiomyocytes exit the cell cycle and undergo terminal differentiation. I examined the transcriptional profiles of MoNucs and BiNucs at developmental timepoints before, during, and after this neonatal transition period. We chose these timepoints to gain insight into how the two cardiomyocyte populations diverge and how their processes of cell cycle exit and maturation may differ. Our data revealed that MoNucs and BiNucs are most distinct during the neonatal period, as these subsets begin to diverge. At P7, binucleation was associated with the termination of a proliferation-associated gene expression program in exchange for a mature cardiomyocyte gene expression program. While this programmatic switch has long been associated with the neonatal period, our findings show that by P7, only BiNucs have begun to undergo this shift, while MoNucs remain transcriptionally immature. While our data show that MoNucs eventually assume a similar mature gene expression program, it appears to do so at a later time, and not as a result of binucleation. These findings raise the possibility that the mechanism that couples binucleation to the observed transcriptional shift also contributes to the increased loss of proliferative competency observed in BiNucs.

E2f target genes comprise a large portion of the most dramatically down-regulated genes in P7 BiNucs, some of which remain down-regulated in adult BiNucs. The E2f transcription factor family is known to regulate the expression of genes required

to initiate DNA synthesis (Johnson et al., 1993). While cardiomyocytes continue to undergo hypertrophic growth after the neonatal maturation period, the S phase is the earliest phase of the cell cycle they do not enter under physiological conditions. E2f activity is known to be regulated by Rb, and this interaction can have temporary, as well as long term control over entry into S phase (Harrington et al., 1998; Lundberg and Weinberg, 1998; Nevins, 1992). Rb mediated silencing of E2f target genes is involved in irreversible exit of the cell cycle during senescence, leaving cells unable to respond to proliferative stimuli (Narita et al., 2003). While the phosphorylation state of Rb dictates temporary repression of S phase entry during the cell cycle, other post-translational modifications to Rb regulate its ability to irreversibly terminate the cell cycle (Kwon et al., 2017; Markham et al., 2006; Saddic et al., 2010). Previous work has also shown that Rb family members are required for cell cycle exit of cardiomyocytes during the postnatal period (MacLellan et al., 2005). This offers an intriguing potential mechanism by which the binucleation process could be coupled to irreversible cell cycle exit.

We knocked out Rb in vitro in neonatal cardiomyocytes to examine its role in binucleation and the depletion of E2f target genes we observed in P7 BiNucs. While the loss of Rb family members did not result in a difference in the ratio of BiNucs to MoNucs, it did result in increased expression of E2f target genes depleted in P7 BiNucs. This places Rb downstream of binucleation and shows that in neonatal cardiomyocytes, Rb is required for down-regulating E2f target gene expression.

In Chapter 3 of this dissertation, I showed that we could alter the ratio of BiNucs to MoNucs during both the embryonic and neonatal periods by knocking out Ect2 in the heart. By altering the ratio of BiNucs to MoNucs during the neonatal maturation period, we demonstrated that increased binucleation at P3 led to decreased expression of E2f target genes. This data supports the hypothesis that Rb mediated silencing of E2f target genes during the neonatal period is a direct result of binucleation. Recent work from Hirose *et al.* further supports the direct connection we observed between binucleation and E2f target gene expression. This work shows that increasing the percentage of diploid MoNucs by expression of a dominant negative thyroid hormone receptor-α is associated with the upregulation of E2f signaling and downregulation of oxidative phosphorylation gene expression (Hirose et al., 2019).

We also used our Ect2 knockout model to show a direct connection between binucleation and regeneration after injury in the murine heart. Increased binucleation during the neonatal period was accompanied by impaired regeneration after ligation of the left anterior descending artery. This data suggests that the loss of regenerative competency is a result of the binucleation process.

4.2 FUTURE DIRECTIONS

In work detailed in this dissertation, I aimed to investigate a link between binucleation and loss of ability to re-enter the cell cycle. Over the last few years, several

new reports have shown that this connection is biologically meaningful, and it has quickly become an important focus in efforts to modulate the regenerative abilities of the heart. The work presented in this dissertation begins to fill in details of the mechanism that connects binucleation to loss of regenerative capacity and, in doing so, raises several new exciting questions and possibilities. It is my hope that the questions outlined below are included among those focused on in future work.

As a result of binucleation, does Rb mediate epigenetic changes responsible for the loss of proliferative competency?

The data presented in Chapters 2 and 3 of this dissertation point to a key role for the Rb/E2f pathway in mediating the link between binucleation and loss of proliferative competency. This possibility is supported by the known roles of the Rb/E2f pathway in regulating permanent cell cycle exit. In senescent cells, regulation of irreversible cell cycle exit by Rb includes the recruitment of chromatin-modifying proteins that alter the architecture of E2f target genes (Blais et al., 2007; Frolov and Dyson, 2004). CpG methylation changes and histone modifications to E2f target genes are also known to occur during the process of cardiomyocyte maturation (Gilsbach et al., 2018; Sdek et al., 2011). Recent work showed that E2f transcription factor networks are among those that undergo extensive chromatin remodeling during the postnatal period and therefore fail to reactivate in adult cardiomyocytes after injury (Quaife-Ryan et al., 2017). Therefore, our

data, together with our current understanding of the Rb/E2f pathway, strongly suggests that Rb may mediate epigenetic changes as a result of binucleation. This offers an intriguing explanation for the results presented in this dissertation, and future work will be necessary to examine this possibility.

What is the functional relevance of the differences we observed between adult MoNucs and BiNucs?

We observed that adult MoNucs and BiNucs retain remnants of some of the differences established during the neonatal period, including differences in E2f target gene expression. Rb mediated differences in the chromatin state of E2f target genes would not only provide an explanation for the differences in proliferative competencies observed between adult MoNucs and BiNucs, but it would also offer a potential explanation for the modest transcriptional differences we observed in E2f target genes between Adult MoNucs and BiNucs. These minor differences in transcript levels of genes that are largely not expressed in this context may not be responsible for functional differences but instead be a reflection of epigenetic differences between the two cell types.

Furthermore, we observed by electron microscopy that adult MoNucs and BiNucs appear to have different densities of glycogen granules. This suggests that MoNucs and

BiNucs may have differences in energy utilization or storage. Future work will be necessary to better understand whether there are indeed metabolic differences between adult MoNucs and BiNucs. Furthermore, if there are differences, it remains to be determined whether they contribute to discrepancies in proliferative competency.

Is a specific set of conditions required to pair the binucleation process to loss of proliferative competency?

Interestingly, induced binucleation via loss of Ect2 led to E2f target gene inhibition at P3 but not at E10.5. We also did not see the same degree of a transcriptional switch in BiNucs at E18.5 compared to BiNucs at P7. Taken together, this suggests that conditions present during the neonatal period, but not the embryonic period, may act to couple binucleation with depletion of E2f target genes. Previous research suggests that the increase in environmental oxygen following birth results in DNA damage by reactive oxygen species. These events have been proposed to initiate the cell cycle exit of cardiomyocytes (Puente et al., 2014). DNA damage-associated cell cycle exit has been observed to be mediated by methylated or acetylated Rb (Markham et al., 2006; Saddic et al., 2010). Perhaps these events must occur in order for binucleation to be paired to the transcriptional switch we observed to occur during the neonatal but not embryonic period. Future work would be needed to examine whether a set of upstream conditions are required for binucleation to result in the transcriptional shift we observed. The answer to this question may offer valuable insight into how these events are linked and whether

they could be unlinked for the purposes of increasing the proliferative competency of cardiomyocytes.

How do our results apply to the human heart?

While a majority of adult murine cardiomyocytes are binucleated, the majority of adult cardiomyocytes in the human heart are thought to be mononucleated and polyploid (Bergmann et al., 2011; Brodsky et al., 1980). Therefore, the applicability of our findings to the human heart remains to be determined. However, the processes resulting in binucleation and polyploidy share similarities, and both can result from failed cell division, whether at the karyokinesis stage or the cytokinesis stage. Karyokinesis and cytokinesis are tightly coupled processes and are orchestrated by a shared group of molecular regulators (Jeyaprakash et al., 2007; McCollum, 2004). Therefore, it is possible that whether destined to become polyploid or binucleated, human and mouse cardiomyocytes share similar molecular mechanisms responsible for, and in response to, failure of cardiomyocytes to complete cell division. First, however, it should be determined whether mononucleated diploid cardiomyocytes in the human heart retain increased proliferative and regenerative competency compared to polyploid and binucleated cardiomyocytes. Work in zebrafish shows that induced binucleation and polyploidy impairs cardiac regeneration, and we showed that this holds true in the mouse heart as well. This would suggest that the link between binucleation or polyploidy and

loss of proliferative competency is conserved over evolution, but future experiments will be necessary to confirm whether this is the case.

4.3 CONCLUDING REMARKS

In this dissertation, I described a novel method to separate mononucleated and binucleated cardiomyocytes, which allowed for the first characterization of the differences between these two cell types. The data presented here provide evidence of a direct link between the binucleation process and the termination of a transcriptional program associated with proliferation. Furthermore, this analysis suggests that an E2f/Rb transcriptional network is centrally involved in the divergence of mononucleated and binucleated cardiomyocytes. This work suggests a potential mechanism by which binucleation may result in loss of regenerative capacity and provides a tool that will allow for further investigations to build on these findings.

CHAPTER 5: METHODS AND MATERIALS

5.1 EXPERIMENTAL MODEL AND SUBJECT DETAILS

Mice

$R26R^{EYFP}$ (Jackson Labs; cat# 006148) (Srinivas et al., 2001), $ROSA26^{FLPe}$ (Jackson Labs; cat# 009086) (Farley et al., 2000), $Nkx2.5^{cre}$ (Jackson Labs; cat# 024637) (Stanley et al., 2002), and $Mlc2v^{cre}$ (Jackson Labs; cat# 029465) (Chen et al., 1998) mice were purchased from Jackson Labs and have been previously described. To generate the $Ect2^{flox/flox}$ allele, cryopreserved sperm from the $Ect2^{tm1a(EUCOMM)Wtsi}$ mouse line was purchased from the Institut Clinique de la Souris (Illkirch, France). The mouse line was derived through in-vitro fertilization by the Transgenic and Chimeric Mouse Facility at the University of Pennsylvania. The resulting mouse was then bred with the $ROSA26^{FLPe}$ allele to remove the neomycin cassette and generate a conditional allele with LoxP sites flanking exon 13 (Figure 5.1). For cardiomyocyte sorting experiments, Adult (8-13 weeks), P7, or E18.5 $Mlc2v^{cre/+}$:$R26R^{EYFP/+}$ offspring were generated by breeding female $R26R^{EYFP/EYFP}$ mice with $Mlc2v^{cre/+}$ males. For Ect2 experiments, $Ect2^{flox/flox}$ mice were bred to either $Mlc2v^{cre/+}$ or $Nkx2.5^{cre/cre}$ to generate mice heterozygous for both alleles. Resulting mice were then bred with $Ect2^{flox/+}$ mice to generate litters used in experiments. A mix of male and female age-matched and litter-matched healthy mice were used for all experiments. No animals were used for more than one experiment. Animals were housed in breeding pairs or with sex-matched littermates in the small animal vivarium at the

Smilow Center for Translational Research at the Perelman School of Medicine and maintained in a 12-h light, 12-h dark cycle with unlimited access to food and water. DNA isolation for genotyping was performed by digesting tails in 50 µL Tris-EDTA, pH8 for 5 minutes at 95°C followed by the addition of 47 µL Tris-EDTA with 3 µL of a 10 mg/ml stock of Proteinase K. The mixture was then incubated for 3 hours at 55°C followed by 5 minutes at 95°C. Genotyping was performed using the primers in Table 5.1. All animal procedures were approved by the University of Pennsylvania Institutional Animal Care and Use Committee under protocol #806345.

5.2 LABORATORY METHODS

Isolation of Mouse Cardiomyocytes

Isolation of Adult Cardiomyocytes

Cardiomyocytes were isolated from mice aged 8-13 weeks using a protocol modified from methods previously described (Judd et al., 2016; Robison et al., 2016; Tian et al., 2015). Buffers were prepared on the day of isolation as follows. Cell Isolation Buffer (CIB): 130 mM NaCl (Sigma; S6191), 1 mM Lactic acid (Sigma; L1750), 5.4 mM KCl (Sigma; P3911), 25 mM HEPES (Bioworld; 0820000-3), 0.50 mM $MgCl_2$ (Sigma; M9272), 0.33 mM NaH_2PO_4 (Sigma; S9638), 22 mM Glucose (Sigma; 16301), 20 mM Creatine Monohydrate (GNC; 350526), brought to pH 7.4 with 10M NaOH. 10X CIB stock excluding Glucose, Creatine, and NaOH was previously prepared and frozen in

aliquots; Digestion buffer: CIB with 60 U/mL Collagenase Type II (Worthington; LS004176) and 0.025 mg/mL Protease Type XIV (Sigma; P5147); Dissociation Buffer: CIB with 1 mg/mL BSA (Omnipor; 2960). Mice were injected with 100 USP units Heparin (Abraxis; 401586B) 25 minutes prior to removal of the heart. Mice were terminally anesthetized with Isoflurane, and the heart was removed and placed in ice-cold CIB. The heart was cannulated via the aorta, secured with 5-0 silk suture, and mounted on a Langendorf apparatus. The heart was then perfused with CIB for 3 min at a temperature of 37°C and a constant flow rate of 3 ml/min, followed by perfusion with Digestion Buffer for 14 minutes. The ventricles were then removed from the Langendorf apparatus and placed in Dissociation Buffer at a temperature of 37°C and gently teased apart with forceps. Tissue was then triturated with a transfer pipette, and the cell suspension was passed through a 100 µm cell strainer. To begin gradually adding back calcium, an equal volume of Dissociation Buffer supplemented with 200 µM Ca^{2+} was then added dropwise to the cell suspension. Cardiomyocytes were enriched by centrifugation at 300 RPM for 3 min and resuspended in Dissociation Buffer supplemented with 250 µM Ca^{2+}. Cardiomyocytes were then allowed to settle by gravity sedimentation for 20 minutes at 37°C and resuspended in 4 mL Dissociation Buffer with 500 µM Ca^{2+}.

Isolation of P7 Cardiomyocytes

Buffers were prepared on the day of isolation as follows. Cell Isolation Buffer (CIB) was the same as used for isolation of adult cardiomyocytes; P7 Digestion Buffer: CIB with 506 U/mL Collagenase Type II and 0.52 mg/mL Trypsin (Fisher; J63993, 1:250); P7 Dissociation Buffer: CIB with 506 U/mL Collagenase Type II and 0.52 mg/mL Trypsin, 10% Horse Serum (Gibco; 16050), 5% Fetal Bovine Serum (Gibco; 10437); P7 Sort Buffer: CIB with 0.66% Horse Serum, and 0.33% Fetal Bovine Serum. Hearts were removed from 7-day-old mice and placed in ice-cold CIB. YFP+ hearts were identified and used for cell isolation. Under a dissection microscope, atria and extraneous tissue were removed, and ventricles were cut into fourths. Each heart was then placed in 2 mL P7 Digestion Buffer and incubated for 30 minutes at 37°C with rocking. Each heart was then transferred to 2 mL P7 Dissociation Buffer supplemented with 60 μM Ca^{2+}, where it was triturated with a transfer pipette followed by a 1000 μL pipette tip. Cell suspensions were then combined and passed through a 70 μm cell strainer. The cell suspension was then centrifuged twice for 5 minutes at 500 RPM and resuspended first in P7 Dissociation Buffer supplemented with 140 μM Ca^{2+}, then in 4 mL P7 Sort Buffer supplemented with 240 μM Ca^{2+}. Vybrant™ DyeCycle™ Violet was added to the cell suspension at 1 μL/mL, and cells were incubated at 37°C for 30 minutes prior to FACS.

Isolation of E18.5 Cardiomyocytes

Buffers were prepared on the day of isolation as follows. E18.5 Digestion Buffer: HBSS (Gibco; 14170) with 10 mM HEPES (Invitrogen; 15630), 0.54 mM EDTA (Invitrogen; 15575) and 2 mg/mL Trypsin; E18.5 Dissociation Buffer: HBSS with 10mM HEPES, 10% Horse Serum, 5% Fetal Bovine Serum; E18.5 Sort Buffer: Opti-MEM (Gibco; 31985) with 0.66% Horse Serum, and 0.33% Fetal Bovine Serum. Time pregnant females were euthanized by CO_2 inhalation. Embryos were removed, and hearts were excised and placed in ice-cold HBSS. YFP+ hearts were identified and used for cell isolation. Under a dissection microscope, atria and extraneous tissue were removed, and ventricles were splayed open. Each heart was then placed in 2 mL E18.5 Digestion Buffer and incubated for 10 minutes at 37°C with rocking. Each heart was then transferred in a drop of Digestion buffer to a well of a 12 well plate and incubated for 30 minutes. 2 mL E18.5 Dissociation Buffer was then added to each well, and the heart was triturated with a 1000 µL pipette tip. Cell suspensions were then combined and passed through a 70 µm cell strainer. The cell suspension was then centrifuged for 5 minutes at 500 RPM and resuspended in 4 mL E18.5 Sort Buffer. Vybrant™ DyeCycle™ Violet was added to the cell suspension at 1 µL/mL, and cells were incubated at 37°C for 30 minutes prior to FACS.

Sorting Mononucleated and Binucleated Cardiomyocytes by FACS

Vybrant™ DyeCycle™ Violet (Invitrogen; V35003) was added to cell suspensions at 1 µL/mL and incubated at 37°C for 30 minutes prior to FACS. Cell sorting was performed on a MoFlo Astrios EQ (Beckman Coulter) at room temperature. Embryonic and neonatal cardiomyocytes were sorted using a 100 um nozzle, while adult cardiomyocytes were sorted using a 150 um nozzle with a maximum pressure difference of 1. Cardiomyocytes from $Mlc2v^{Cre}$:$R26R^{EYFP}$ mice were gated on YFP presence with a 488 nm laser. Nucleation was gated on the height and width of the signal from a 405 nm laser as described above. Prior to collection, 50-100 cells within each gate were sorted onto a slide and imaged with the DAPI, GFP, and transmitted light channels of an EVOS FL Auto imaging system microscope (ThermoFisher; AMAFD1000) to ensure correct separation of mononucleated and binucleated cells. If necessary, gates were adjusted until the targeted cells were correctly identified. For RNA, an equal number of mononucleated and binucleated cardiomyocytes were sorted into Trizol-LS (LifeTech; 10296028).

RNA Isolation for RNA-seq and qPCR

RNA was isolated by phenol-chloroform extraction followed by precipitation with 75% Ethanol. RNA was then purified using the RNeasy micro Kit (Qiagen; 74004) as follows. A solution containing precipitated RNA was applied to an RNeasy MinElute Spin Column, and washes were done according to the manufacturer's protocol. RNA was then

eluted in 20 µL H2O. RNA to be sequenced was tested for integrity via Bioanalyzer using the RNA 6000 Pico Kit (Agilent; 5067). RNA for qPCR was quantified using a Nanodrop One (Thermo), and cDNA was generated using the Superscript IV First-Strand Synthesis System (ThermoFisher; 18090050). Quantitative Real-Time PCR was performed on a QuantStudio 7 Flex with Power SYBR Green PCR Mastermix (Applied Biosystems; 4367659). QPCR primer sequences are listed in Table 4.2.

Surgical Procedures

To induce MI in neonatal mice, we permanently ligated the LAD artery on postnatal day 1 (P1) as previously described (Leach et al., 2017). To minimize stress and reduce the likelihood of the pups being rejected by the nursing dam, only half of the litter was removed prior to commencing surgery. Pups were housed in an incubation chamber to provide warmth throughout and after the surgical procedure. The dam was housed away from the operating table during the procedure. P1 mice were anesthetized by cooling on ice. Once the appropriate plane of anesthesia is reached, the neonate was removed from the ice for the surgical procedure. Appropriate anesthesia was recognized by a lack of breathing, movement, and reflexes. The pup was placed atop a firm operating surface in the supine position. Forelimbs and tail were held in position using masking tape. A dissecting microscope with a fibro-optic light was used for visualization throughout the surgery. A lateral skin incision was then made on the left side of the chest, just below the

insertion of the left forelimb, using fine scissors and forceps. Blunt dissection was used to expose the ribs, and a lateral thoracotomy was performed at the fourth intercostal space by blunt dissection of the intercostal muscles following skin incision. The left anterior descending coronary artery (LAD) was identified under the microscope. 8-0 nylon suture was then sutured across the LAD and permanently ligated. The visualization of the whitish color of the left ventricular apex assured the effective ligation of LAD. Following the LAD ligation, the thoracotomy was closed by re-approximating the ribs using a 6-0 non-absorbable suture. The skin incision was then closed using Vetbond, a skin adhesive glue. The entire procedure took less than 10 minutes per mouse. The instruments were sterilized between procedures using a hot bead sterilizer. After surgery, pups were brought back to body temperature by placing them in a 33C incubator for 20-30 minutes.

In vitro Experiments

Cardiomyocytes were isolated from $Rb^{flox/flox}$;$p130^{flox/flox}$;$p107^{-/-}$ pups at postnatal day 1. Buffers and protocol were as described for isolating E18.5 cardiomyocytes with the following modifications. Rinse buffer: DMEM with 10% Horse Serum, 5% Fetal Bovine Serum, 1% Pen/Strep. High Serum Culture Media: Opti-MEM with 10% Horse Serum, 5% Fetal Bovine Serum, 1% Pen/Strep. Low Serum Culture Media: Opti-MEM with 0.7% Horse Serum, 0.3% Fetal Bovine Serum, 1% Pen/Strep. Each heart was placed in 2 mL Digestion Buffer and incubated overnight at 4°C with rocking instead of 10 minutes

at 37°C. Following dissociation, cell suspensions were washed with Rinse Media, then resuspended in High Serum Culture media and passed through a 70 μm cell strainer. Fibroblasts were depleted by plating cell suspensions for 2 hours on cell culture plastic. Cell suspensions were then collected, and cells counted with a hemocytometer. 75,000 cells in High Serum Culture Media were plated in per well of a 48 well plate, precoated overnight with 100 □g/mL laminin. The following day, each well of cells was treated with 5x10^6 PFU of adenovirus expressing either GFP (Ad-GFP) (Vector Biolabs; 1060) or both Cre recombinase and GFP (Ad-Cre-GFP) (Vector Biolabs; 1700). The morning after adenoviral infection, media was changed to Low Serum Culture Media for 24 hours to inhibit the growth of fibroblasts. 36 hours after adenoviral infection, media was changed back to High Serum culture media, and cells were cultured for an additional 36 hours. 72 hours after adenoviral infection, cells were harvested in Trizol for RNA as described above or fixed for staining to quantify nucleation.

Histology and Immunostaining

Single-cell suspensions of cardiomyocytes were fixed in 4% PFA and permeabilized in PBS with 0.5% TritonX-100. SEA BLOCK blocking buffer (ThermoFisher; 37527) was used for blocking, diluting antibodies, and washes. Cells were incubated with primary antibody overnight at 4°C, followed by the secondary antibody for 1 hour at room temperature. Cells were then incubated with DAPI, pelleted, resuspended in ProLong

Diamond Antifade Mountant (ThermoFisher; P36961), and mounted on slides. Images were acquired with the Nikon Eclipse Ni-E microscope, and mononucleated and binucleated cells were counted using Fiji Software. Histology was performed by members of the Penn Cardiovascular Institute's Histology and Gene Expression Core Facility. For Histology, tissues were fixed in 4% paraformaldehyde, dehydrated through a series of ethanol washes, and embedded in paraffin. Tissue was sectioned at 6 μm intervals and stained with either *hematoxylin* and eosin, Masson's trichrome, or by immunostaining. Primary antibody information and concentrations used are listed in Table 4.3.

Electron Microscopy

Cardiomyocytes for electron microscopic examination were sorted directly into fixative containing 2.5% glutaraldehyde, 2.0% paraformaldehyde in 0.1M sodium cacodylate buffer, pH 7.4, overnight at 4°C. After subsequent buffer washes, the samples were post-fixed in 2.0% osmium tetroxide for 1 hour at room temperature and rinsed in DH_2O prior to en bloc staining with 2% uranyl acetate. After dehydration through a graded ethanol series, the tissue was infiltrated and embedded in EMbed-812 (Electron Microscopy Sciences, Fort Washington, PA). Thin sections were stained with uranyl acetate and lead citrate and examined with a JEOL 1010 electron microscope fitted with a Hamamatsu digital camera and AMT Advantage image capture software.

5.3 QUANTIFICATION AND STATISTICAL ANALYSIS

Statistical Analysis

Data are reported as Mean ± SEM. Statistical analysis was performed in Prism 7 for Mac. Unless otherwise specified, an unpaired Student's t-test was used to compare two experimental groups. For injury studies, a Mann-Whitney U test was used. Data were considered significant if $p < 0.05$.

Quantification of Scar Size

Scar size was measured as the percent fibrosis of the left ventricle myocardium from the site of the suture to the apex using MIQuant, an automated image segmentation open-source code for MATLAB (Nascimento et al., 2011). The average of two independent measurements of scar size is reported. The initial measurement was not obtained blind; to ensure reproducibility, a second investigator measured scar size blind to genotype.

RNA-Sequencing and Analysis

Library prep was conducted using Illumina truSeq stranded mRNA kit and Clontech SMARTer RNA-seq amplification kit. Fastq files were assessed for quality control using the FastQC program. Fastq files were aligned against the mouse reference genome (mm9) using the STAR aligner (Dobin et al., 2013). Duplicate reads were flagged using the

MarkDuplicates program from Picard tools. Per gene read counts for Ensembl (v67) gene annotations were computed using the R package with duplicate reads removed. Gene counts represented as counts per million (CPM) were first nominalized using TMM method in the edgeR R package, and genes with 25% of samples with a CPM < 1 were removed and deemed low expressed. The data were transformed using the VOOM function from the limma R package (Law et al., 2014). Differential gene expression was performed as a paired analysis between mono-nuclear and bi-nuclear samples using limma. To perform the pair-wise test, the subject correlation was first computed using duplicate Correlation() function, and the linear model was then fit using the subject as a blocking variable and adjusting for the subject correlation. Given the small sample size of the experiment, we employed the empirical Bayes procedure as implemented in limma to adjust the linear fit and calculate p-values. p-values were adjusted for multiple comparisons using the Benjamini-Hochberg procedure. Heatmaps and PCA plots were generated in R. Gene Ontology enrichment analysis was performed using the ToppGene Suite (https://toppgene.cchmc.org/) (Chen et al., 2009).

Data and Code Availability

The sequencing data in this manuscript are available on GEO through the accession number: GSE140851

Figure 5.1 Generation and genotyping of the floxed Ect2 allele

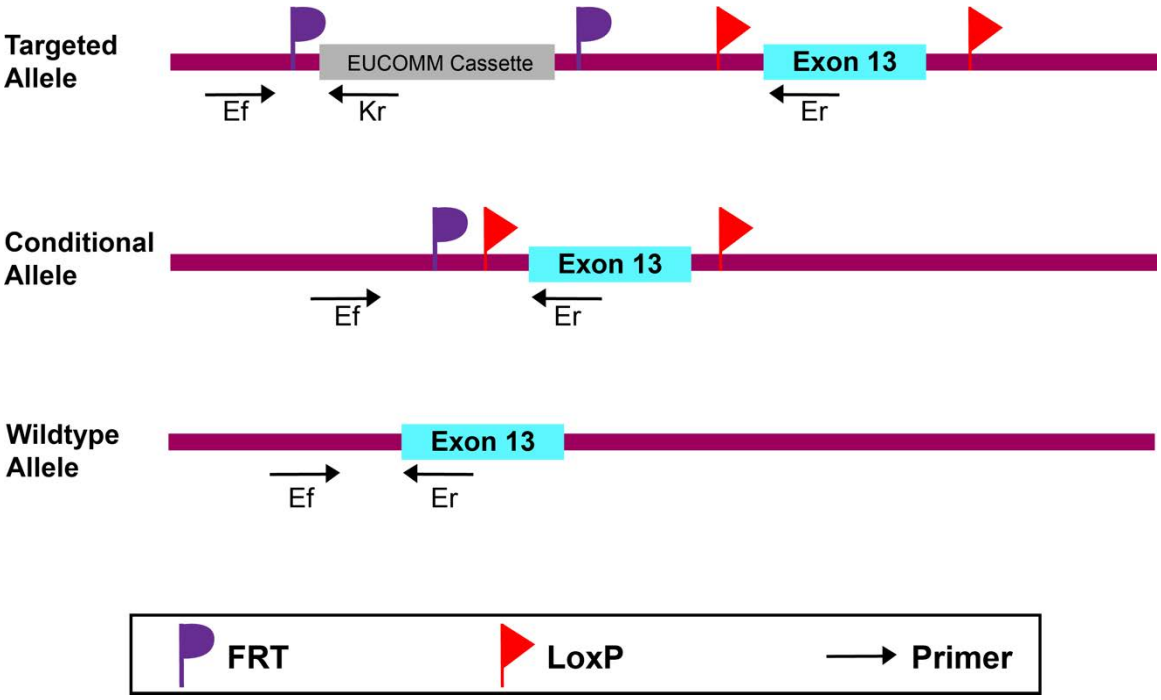

Figure 5.1 Generation and genotyping of the floxed Ect2 allele

A mouse line containing the targeted allele was derived through in-vitro fertilization by the Transgenic and Chimeric Mouse Facility at the University of Pennsylvania. Genotyping of tails from mice containing the targeted allele with the Kr and Ef primers resulted in amplification of a 318 bp PCR product. Once the neomycin cassette is removed by breeding to a ROSA26^{FLPe} allele, genotyping of the conditional allele with the Ef and Er primers will generate a PCR product of 502 bp whereas the wild type allele will generate and PCR product of 402 bp. Figure was adapted from literature provided by the Institut Clinique de la Souris.

Table 5.1 Genotyping primer sequences

Primer	Sequence
Ect2-Ef	ATTGTCACTCATGCTAGGGAGGTGC
Ect2-Er	CGTGTGAAGTTCTAGGCTCAACCACAA
Ect2- Kr	CCAACAGCTTCCCCACAACGG
$Mlc2v^{cre}$ Fwd	CCAGGGGAGAGGTATTTATTGTTCC
$Mlc2v^{cre}$ Rev	CCAGGTATGCTCAGAAAACGCC
$Nkx2.5^{cre}$ Fwd	CGTTTTCTGAGCATACCTGGA
$Nkx2.5^{cre}$ Rev	ATTCTCCCACCGTCAGTACG
$R26R^{EYFP}$ mut Fwd	AAGGGAGCTGCAGTGGAGTA
$R26R^{EYFP}$ mut Rev	CCGAAAATCTGTGGGAAGTC
$R26R^{EYFP}$ wt Fwd	ACATGGTCCTGCTGGAGTTC
$R26R^{EYFP}$ wt Rev	GGCATTAAAGCAGCGTATCC

Table 5.2 qPCR primer sequences

Gene	Sequence
E2f1 Fwd	GGGAGAAGTCACGCTATGAAACCT
E2f1 Rev	ATGTCATAGATGCGCCGTTTCTGC
Mcm2 Fwd	AACTGTAGCAAGTGCAACTTTGT
Mcm2 Rev	GCGGATACGTTGGTAGTTCTGAT
Ccne2 Fwd	ATGTCAAGACGCAGCCGTTTA
Ccne2 Rev	GCTGATTCCTCCAGACAGTACA
Top2a Fwd	CGAGCAAGAAAGCAAAGGG
Top2a Rev	CTTAATTGGCTTCCTCGCC
Ccne1 Fwd	AGCGAGGATAGCAGTCAGCC
Ccne1 Rev	GGTGGTCTGATTTTCCGAGG
Mcm6 Fwd	CCTGTGAATAGGTTCAACGGC
Mcm6 Rev	CATTTTCCTGAGGTGGAGCAC
Cdt1 Fwd	ACAGCCGGGCAAGATCCCCT
Cdt1 Rev	GGCTCCCAACTTCCGTGCCC
Rfc2 Fwd	CTGCCGTGGGTTGAAAAATACA
Rfc2 Rev	CAGAGGATGCTGGTTGTCTTG
Pcna Fwd	TTTGAGGCACGCCTGATCC
Pcna Rev	GGAGACGTGAGACGAGTCCAT
Cdk5 Fwd	CCCTGAGATTGTGAAGTCATTCC
Cdk5 Rev	CCAATTTCAACTCCCCATTCCT
Myh7 Fwd	GAGCCTTGGATTCTCAAACG
Myh7 Rev	GTGGCTCCGAGAAAGGAAG
Rb1 Fwd	TGCATCTTTATCGCAGCAGTT
Rb1 Rev	GTTCACACGTCCGTTCTAATTTG
Necdin Fwd	GGCGCTCAACAACCGTATG
Necdin Rev	CTCGGTGATTATCTTCCTCACG
Cenpf Fwd	GCACAGCACAGTATGACCAGG
Cenpf Rev	CTCTGCGTTCTGTCGGTGAC
Ect2 Exon13 Fwd	TACTCCAGTTCCTCCAAAGCAG
Ect2 Exon13 Rev	GTCCTTCTTCTTCTAAGGGCACC
Gapdh Fwd	TGCACCACCAACTGCTTAGC
Gapdh Rev	GGCATGGACTGTGGTCATGAG

Table 5.3 Primary antibodies used for immunostaining

Antibody	Species	Company	Catalog #	Dilution
Sarcomeric α-Actinin	Mouse	Sigma	A7811	1:100
Troponin T-C	Goat	Santa Cruz	sc-8121	1:25
GFP	Goat	Abcam	ab6673	1:500
Phospho-Histone H3	Rabbit	Cell Signaling	9701	1:150
Aurora B Kinase	Rabbit	Abcam	ab2254	1:1000
Ki67	Rabbit	abcam	ab16667	1:50
PCM1	Rabbit	Sigma	HPA023370	1:100

BIBLIOGRAPHY

Agah, R., Kirshenbaum, L.A., Abdellatif, M., Truong, L.D., Chakraborty, S., Michael, L.H., and Schneider, M.D. (1997). Adenoviral delivery of E2F-1 directs cell cycle reentry and p53-independent apoptosis in postmitotic adult myocardium in vivo. The Journal of clinical investigation *100*, 2722-2728.

Ahuja, P., Perriard, E., Perriard, J.C., and Ehler, E. (2004). Sequential myofibrillar breakdown accompanies mitotic division of mammalian cardiomyocytes. Journal of cell science *117*, 3295-3306.

Beauchamp, J.R., Morgan, J.E., Pagel, C.N., and Partridge, T.A. (1999). Dynamics of myoblast transplantation reveal a discrete minority of precursors with stem cell-like properties as the myogenic source. The Journal of cell biology *144*, 1113-1122.

Beltrami, A.P., Barlucchi, L., Torella, D., Baker, M., Limana, F., Chimenti, S., Kasahara, H., Rota, M., Musso, E., Urbanek, K.*, et al.* (2003). Adult cardiac stem cells are multipotent and support myocardial regeneration. Cell *114*, 763-776.

Bergmann, O., Bhardwaj, R.D., Bernard, S., Zdunek, S., Barnabe-Heider, F., Walsh, S., Zupicich, J., Alkass, K., Buchholz, B.A., Druid, H.*, et al.* (2009). Evidence for cardiomyocyte renewal in humans. Science *324*, 98-102.

Bergmann, O., Zdunek, S., Alkass, K., Druid, H., Bernard, S., and Frisen, J. (2011). Identification of cardiomyocyte nuclei and assessment of ploidy for the analysis of cell turnover. Experimental cell research *317*, 188-194.

Bersell, K., Arab, S., Haring, B., and Kuhn, B. (2009). Neuregulin1/ErbB4 signaling induces cardiomyocyte proliferation and repair of heart injury. Cell *138*, 257-270.

Blais, A., van Oevelen, C.J., Margueron, R., Acosta-Alvear, D., and Dynlacht, B.D. (2007). Retinoblastoma tumor suppressor protein-dependent methylation of histone H3 lysine 27 is associated with irreversible cell cycle exit. The Journal of cell biology *179*, 1399-1412.

Braunwald, E., and Bonow, R.O. (2012). Braunwald's heart disease : a textbook of cardiovascular medicine, 9th edn (Philadelphia: Saunders).

Brodsky, W.Y., Arefyeva, A.M., and Uryvaeva, I.V. (1980). Mitotic polyploidization of mouse heart myocytes during the first postnatal week. Cell and tissue research *210*, 133-144.

Celermajer, D.S., Sholler, G.F., Howman-Giles, R., and Celermajer, J.M. (1991). Myocardial infarction in childhood: clinical analysis of 17 cases and medium term follow up of survivors. British heart journal *65*, 332-336.

Chen, J., Bardes, E.E., Aronow, B.J., and Jegga, A.G. (2009). ToppGene Suite for gene list enrichment analysis and candidate gene prioritization. Nucleic acids research *37*, W305-311.

Chen, J., Kubalak, S.W., Minamisawa, S., Price, R.L., Becker, K.D., Hickey, R., Ross, J., Jr., and Chien, K.R. (1998). Selective requirement of myosin light chain 2v in embryonic heart function. The Journal of biological chemistry *273*, 1252-1256.

Chong, J.J., Yang, X., Don, C.W., Minami, E., Liu, Y.W., Weyers, J.J., Mahoney, W.M., Van Biber, B., Cook, S.M., Palpant, N.J.*, et al.* (2014). Human embryonic-stem-cell-derived cardiomyocytes regenerate non-human primate hearts. Nature *510*, 273-277.

Dobin, A., Davis, C.A., Schlesinger, F., Drenkow, J., Zaleski, C., Jha, S., Batut, P., Chaisson, M., and Gingeras, T.R. (2013). STAR: ultrafast universal RNA-seq aligner. Bioinformatics *29*, 15-21.

Drenckhahn, J.D., Schwarz, Q.P., Gray, S., Laskowski, A., Kiriazis, H., Ming, Z., Harvey, R.P., Du, X.J., Thorburn, D.R., and Cox, T.C. (2008). Compensatory growth of healthy cardiac cells in the presence of diseased cells restores tissue homeostasis during heart development. Dev Cell *15*, 521-533.

Engel, F.B., Schebesta, M., Duong, M.T., Lu, G., Ren, S., Madwed, J.B., Jiang, H., Wang, Y., and Keating, M.T. (2005). p38 MAP kinase inhibition enables proliferation of adult mammalian cardiomyocytes. Genes Dev *19*, 1175-1187.

Engel, F.B., Schebesta, M., and Keating, M.T. (2006). Anillin localization defect in cardiomyocyte binucleation. Journal of molecular and cellular cardiology *41*, 601-612.

Eschenhagen, T., Bolli, R., Braun, T., Field, L.J., Fleischmann, B.K., Frisen, J., Giacca, M., Hare, J.M., Houser, S., Lee, R.T.*, et al.* (2017). Cardiomyocyte Regeneration: A Consensus Statement. Circulation *136*, 680-686.

Farley, F.W., Soriano, P., Steffen, L.S., and Dymecki, S.M. (2000). Widespread recombinase expression using FLPeR (flipper) mice. Genesis (New York, NY : 2000) *28*, 106-110.

Fields, A.P., and Justilien, V. (2010). The guanine nucleotide exchange factor (GEF) Ect2 is an oncogene in human cancer. Advances in enzyme regulation *50*, 190-200.

Frolov, M.V., and Dyson, N.J. (2004). Molecular mechanisms of E2F-dependent activation and pRB-mediated repression. Journal of cell science *117*, 2173-2181.

Gillers, B.S., Chiplunkar, A., Aly, H., Valenta, T., Basler, K., Christoffels, V.M., Efimov, I.R., Boukens, B.J., and Rentschler, S. (2015). Canonical wnt signaling regulates atrioventricular junction programming and electrophysiological properties. Circulation research *116*, 398-406.

Gilsbach, R., Schwaderer, M., Preissl, S., Gruning, B.A., Kranzhofer, D., Schneider, P., Nuhrenberg, T.G., Mulero-Navarro, S., Weichenhan, D., Braun, C.*, et al.* (2018). Distinct epigenetic programs regulate cardiac myocyte development and disease in the human heart in vivo. Nature communications *9*, 391.

Gonzalez-Rosa, J.M., Sharpe, M., Field, D., Soonpaa, M.H., Field, L.J., Burns, C.E., and Burns, C.G. (2018). Myocardial Polyploidization Creates a Barrier to Heart Regeneration in Zebrafish. Dev Cell *44*, 433-446 e437.

Guimaraes-Camboa, N., Stowe, J., Aneas, I., Sakabe, N., Cattaneo, P., Henderson, L., Kilberg, M.S., Johnson, R.S., Chen, J., McCulloch, A.D.*, et al.* (2015). HIF1alpha Represses Cell Stress Pathways to Allow Proliferation of Hypoxic Fetal Cardiomyocytes. Dev Cell *33*, 507-521.

Harrington, E.A., Bruce, J.L., Harlow, E., and Dyson, N. (1998). pRB plays an essential role in cell cycle arrest induced by DNA damage. Proceedings of the National Academy of Sciences of the United States of America *95*, 11945-11950.

Haubner, B.J., Adamowicz-Brice, M., Khadayate, S., Tiefenthaler, V., Metzler, B., Aitman, T., and Penninger, J.M. (2012). Complete cardiac regeneration in a mouse model of myocardial infarction. Aging *4*, 966-977.

Haubner, B.J., Schneider, J., Schweigmann, U., Schuetz, T., Dichtl, W., Velik-Salchner, C., Stein, J.I., and Penninger, J.M. (2016). Functional Recovery of a Human Neonatal Heart After Severe Myocardial Infarction. Circulation research *118*, 216-221.

Heallen, T., Morikawa, Y., Leach, J., Tao, G., Willerson, J.T., Johnson, R.L., and Martin, J.F. (2013). Hippo signaling impedes adult heart regeneration. Development (Cambridge, England) *140*, 4683-4690.

Hirose, K., Payumo, A.Y., Cutie, S., Hoang, A., Zhang, H., Guyot, R., Lunn, D., Bigley, R.B., Yu, H., Wang, J.*, et al.* (2019). Evidence for hormonal control of heart regenerative capacity during endothermy acquisition. Science *364*, 184-188.

Ieda, M., Fu, J.D., Delgado-Olguin, P., Vedantham, V., Hayashi, Y., Bruneau, B.G., and Srivastava, D. (2010). Direct reprogramming of fibroblasts into functional cardiomyocytes by defined factors. Cell *142*, 375-386.

Ikenishi, A., Okayama, H., Iwamoto, N., Yoshitome, S., Tane, S., Nakamura, K., Obayashi, T., Hayashi, T., and Takeuchi, T. (2012). Cell cycle regulation in mouse heart during embryonic and postnatal stages. Development, growth & differentiation *54*, 731-738.

Jacot, J.G., Martin, J.C., and Hunt, D.L. (2010). Mechanobiology of cardiomyocyte development. Journal of biomechanics *43*, 93-98.

Jeyaprakash, A.A., Klein, U.R., Lindner, D., Ebert, J., Nigg, E.A., and Conti, E. (2007). Structure of a Survivin-Borealin-INCENP core complex reveals how chromosomal passengers travel together. Cell *131*, 271-285.

Johnson, D.G., Schwarz, J.K., Cress, W.D., and Nevins, J.R. (1993). Expression of transcription factor E2F1 induces quiescent cells to enter S phase. Nature *365*, 349-352.

Jopling, C., Sleep, E., Raya, M., Marti, M., Raya, A., and Izpisua Belmonte, J.C. (2010). Zebrafish heart regeneration occurs by cardiomyocyte dedifferentiation and proliferation. Nature *464*, 606-609.

Judd, J., Lovas, J., and Huang, G.N. (2016). Isolation, Culture and Transduction of Adult Mouse Cardiomyocytes. Journal of visualized experiments : JoVE.

Kamijo, K., Ohara, N., Abe, M., Uchimura, T., Hosoya, H., Lee, J.S., and Miki, T. (2006). Dissecting the role of Rho-mediated signaling in contractile ring formation. Molecular biology of the cell *17*, 43-55.

Kehat, I., Kenyagin-Karsenti, D., Snir, M., Segev, H., Amit, M., Gepstein, A., Livne, E., Binah, O., Itskovitz-Eldor, J., and Gepstein, L. (2001). Human embryonic stem cells can differentiate into myocytes with structural and functional properties of cardiomyocytes. The Journal of clinical investigation *108*, 407-414.

Kou, C.Y., Lau, S.L., Au, K.W., Leung, P.Y., Chim, S.S., Fung, K.P., Waye, M.M., and Tsui, S.K. (2010). Epigenetic regulation of neonatal cardiomyocytes differentiation. Biochemical and biophysical research communications *400*, 278-283.

Kuhn, B., del Monte, F., Hajjar, R.J., Chang, Y.S., Lebeche, D., Arab, S., and Keating, M.T. (2007). Periostin induces proliferation of differentiated cardiomyocytes and promotes cardiac repair. Nat Med *13*, 962-969.

Kwon, J.S., Everetts, N.J., Wang, X., Wang, W., Della Croce, K., Xing, J., and Yao, G. (2017). Controlling Depth of Cellular Quiescence by an Rb-E2F Network Switch. Cell reports *20*, 3223-3235.

Lahmers, S., Wu, Y., Call, D.R., Labeit, S., and Granzier, H. (2004). Developmental control of titin isoform expression and passive stiffness in fetal and neonatal myocardium. Circulation research *94*, 505-513.

Lavine, K.J., Yu, K., White, A.C., Zhang, X., Smith, C., Partanen, J., and Ornitz, D.M. (2005). Endocardial and epicardial derived FGF signals regulate myocardial proliferation and differentiation in vivo. Dev Cell *8*, 85-95.

Law, C.W., Chen, Y., Shi, W., and Smyth, G.K. (2014). voom: Precision weights unlock linear model analysis tools for RNA-seq read counts. Genome biology *15*, R29.

Leach, J.P., Heallen, T., Zhang, M., Rahmani, M., Morikawa, Y., Hill, M.C., Segura, A., Willerson, J.T., and Martin, J.F. (2017). Hippo pathway deficiency reverses systolic heart failure after infarction. Nature *550*, 260-264.

Li, F., Wang, X., Capasso, J.M., and Gerdes, A.M. (1996). Rapid transition of cardiac myocytes from hyperplasia to hypertrophy during postnatal development. Journal of molecular and cellular cardiology *28*, 1737-1746.

Li, F., Wang, X., and Gerdes, A.M. (1997). Formation of binucleated cardiac myocytes in rat heart: II. Cytoskeletal organisation. Journal of molecular and cellular cardiology *29*, 1553-1565.

Liao, H.S., Kang, P.M., Nagashima, H., Yamasaki, N., Usheva, A., Ding, B., Lorell, B.H., and Izumo, S. (2001). Cardiac-specific overexpression of cyclin-dependent kinase 2 increases smaller mononuclear cardiomyocytes. Circulation research *88*, 443-450.

Lopaschuk, G.D., and Jaswal, J.S. (2010). Energy metabolic phenotype of the cardiomyocyte during development, differentiation, and postnatal maturation. Journal of cardiovascular pharmacology *56*, 130-140.

Lundberg, A.S., and Weinberg, R.A. (1998). Functional inactivation of the retinoblastoma protein requires sequential modification by at least two distinct cyclin-cdk complexes. Molecular and cellular biology *18*, 753-761.

Lunt, S.Y., and Vander Heiden, M.G. (2011). Aerobic glycolysis: meeting the metabolic requirements of cell proliferation. Annual review of cell and developmental biology *27*, 441-464.

MacLellan, W.R., Garcia, A., Oh, H., Frenkel, P., Jordan, M.C., Roos, K.P., and Schneider, M.D. (2005). Overlapping roles of pocket proteins in the myocardium are unmasked by germ line deletion of p130 plus heart-specific deletion of Rb. Molecular and cellular biology *25*, 2486-2497.

Markham, D., Munro, S., Soloway, J., O'Connor, D.P., and La Thangue, N.B. (2006). DNA-damage-responsive acetylation of pRb regulates binding to E2F-1. EMBO reports *7*, 192-198.

Mauritz, C., Schwanke, K., Reppel, M., Neef, S., Katsirntaki, K., Maier, L.S., Nguemo, F., Menke, S., Haustein, M., Hescheler, J.*, et al.* (2008). Generation of functional murine cardiac myocytes from induced pluripotent stem cells. Circulation *118*, 507-517.

Mauro, A. (1961). Satellite cell of skeletal muscle fibers. The Journal of biophysical and biochemical cytology *9*, 493-495.

McCollum, D. (2004). Cytokinesis: the central spindle takes center stage. Current biology : CB *14*, R953-955.

Mohamed, T.M., Stone, N.R., Berry, E.C., Radzinsky, E., Huang, Y., Pratt, K., Ang, Y.S., Yu, P., Wang, H., Tang, S.*, et al.* (2017). Chemical Enhancement of In Vitro and In Vivo Direct Cardiac Reprogramming. Circulation *135*, 978-995.

Murphy, A.M. (1996). Contractile protein phenotypic variation during development. Cardiovascular research *31 Spec No*, E25-33.

Murry, C.E., Reinecke, H., and Pabon, L.M. (2006). Regeneration gaps: observations on stem cells and cardiac repair. Journal of the American College of Cardiology *47*, 1777-1785.

Narita, M., Nunez, S., Heard, E., Narita, M., Lin, A.W., Hearn, S.A., Spector, D.L., Hannon, G.J., and Lowe, S.W. (2003). Rb-mediated heterochromatin formation and silencing of E2F target genes during cellular senescence. Cell *113*, 703-716.

Nascimento, D.S., Valente, M., Esteves, T., de Pina Mde, F., Guedes, J.G., Freire, A., Quelhas, P., and Pinto-do, O.P. (2011). MIQuant--semi-automation of infarct size assessment in models of cardiac ischemic injury. PloS one *6*, e25045.

Nevins, J.R. (1992). E2F: a link between the Rb tumor suppressor protein and viral oncoproteins. Science *258*, 424-429.

Oberpriller, J.O., and Oberpriller, J.C. (1974). Response of the adult newt ventricle to injury. The Journal of experimental zoology *187*, 249-253.

Oparil, S., Bishop, S.P., and Clubb, F.J., Jr. (1984). Myocardial cell hypertrophy or hyperplasia. Hypertension (Dallas, Tex : 1979) *6*, Iii38-43.

Ozkan, J. (2019). Piero Anversa and cardiomyocyte regeneration. European heart journal *40*, 1036-1037.

Papadimou, E., Menard, C., Grey, C., and Puceat, M. (2005). Interplay between the retinoblastoma protein and LEK1 specifies stem cells toward the cardiac lineage. The EMBO journal *24*, 1750-1761.

Pasumarthi, K.B., Nakajima, H., Nakajima, H.O., Soonpaa, M.H., and Field, L.J. (2005). Targeted expression of cyclin D2 results in cardiomyocyte DNA synthesis and infarct regression in transgenic mice. Circulation research *96*, 110-118.

Patterson, M., Barske, L., Van Handel, B., Rau, C.D., Gan, P., Sharma, A., Parikh, S., Denholtz, M., Huang, Y., Yamaguchi, Y.*, et al.* (2017). Frequency of mononuclear diploid cardiomyocytes underlies natural variation in heart regeneration. Nat Genet *49*, 1346-1353.

Piquereau, J., Novotova, M., Fortin, D., Garnier, A., Ventura-Clapier, R., Veksler, V., and Joubert, F. (2010). Postnatal development of mouse heart: formation of energetic microdomains. The Journal of physiology *588*, 2443-2454.

Poolman, R.A., Li, J.M., Durand, B., and Brooks, G. (1999). Altered expression of cell cycle proteins and prolonged duration of cardiac myocyte hyperplasia in p27KIP1 knockout mice. Circulation research *85*, 117-127.

Porrello, E.R., Mahmoud, A.I., Simpson, E., Hill, J.A., Richardson, J.A., Olson, E.N., and Sadek, H.A. (2011). Transient regenerative potential of the neonatal mouse heart. Science *331*, 1078-1080.

Porrello, E.R., and Olson, E.N. (2014). A neonatal blueprint for cardiac regeneration. Stem cell research *13*, 556-570.

Poss, K.D., Wilson, L.G., and Keating, M.T. (2002). Heart regeneration in zebrafish. Science *298*, 2188-2190.

Prats, C., Graham, T.E., and Shearer, J. (2018). The dynamic life of the glycogen granule. The Journal of biological chemistry *293*, 7089-7098.

Puente, B.N., Kimura, W., Muralidhar, S.A., Moon, J., Amatruda, J.F., Phelps, K.L., Grinsfelder, D., Rothermel, B.A., Chen, R., Garcia, J.A., *et al.* (2014). The oxygen-rich postnatal environment induces cardiomyocyte cell-cycle arrest through DNA damage response. Cell *157*, 565-579.

Qian, L., Huang, Y., Spencer, C.I., Foley, A., Vedantham, V., Liu, L., Conway, S.J., Fu, J.D., and Srivastava, D. (2012). In vivo reprogramming of murine cardiac fibroblasts into induced cardiomyocytes. Nature *485*, 593-598.

Quaife-Ryan, G.A., Sim, C.B., Ziemann, M., Kaspi, A., Rafehi, H., Ramialison, M., El-Osta, A., Hudson, J.E., and Porrello, E.R. (2017). Multicellular Transcriptional Analysis of Mammalian Heart Regeneration. Circulation *136*, 1123-1139.

Robison, P., Caporizzo, M.A., Ahmadzadeh, H., Bogush, A.I., Chen, C.Y., Margulies, K.B., Shenoy, V.B., and Prosser, B.L. (2016). Detyrosinated microtubules buckle and bear load in contracting cardiomyocytes. Science *352*, aaf0659.

Saddic, L.A., West, L.E., Aslanian, A., Yates, J.R., 3rd, Rubin, S.M., Gozani, O., and Sage, J. (2010). Methylation of the retinoblastoma tumor suppressor by SMYD2. The Journal of biological chemistry *285*, 37733-37740.

Saggin, L., Gorza, L., Ausoni, S., and Schiaffino, S. (1989). Troponin I switching in the developing heart. The Journal of biological chemistry *264*, 16299-16302.

Schneider, J.L., Suh, Y., and Cuervo, A.M. (2014). Deficient chaperone-mediated autophagy in liver leads to metabolic dysregulation. Cell metabolism *20*, 417-432.

Sdek, P., Zhao, P., Wang, Y., Huang, C.J., Ko, C.Y., Butler, P.C., Weiss, J.N., and Maclellan, W.R. (2011). Rb and p130 control cell cycle gene silencing to maintain the postmitotic phenotype in cardiac myocytes. The Journal of cell biology *194*, 407-423.

Shapiro, H.M. (1985). Practical flow cytometry (New York, N.Y.: A.R. Liss).

Siedner, S., Kruger, M., Schroeter, M., Metzler, D., Roell, W., Fleischmann, B.K., Hescheler, J., Pfitzer, G., and Stehle, R. (2003). Developmental changes in contractility and sarcomeric proteins from the early embryonic to the adult stage in the mouse heart. The Journal of physiology *548*, 493-505.

Soonpaa, M.H., Kim, K.K., Pajak, L., Franklin, M., and Field, L.J. (1996). Cardiomyocyte DNA synthesis and binucleation during murine development. The American journal of physiology *271*, H2183-2189.

Soonpaa, M.H., Koh, G.Y., Pajak, L., Jing, S., Wang, H., Franklin, M.T., Kim, K.K., and Field, L.J. (1997). Cyclin D1 overexpression promotes cardiomyocyte DNA synthesis and multinucleation in transgenic mice. The Journal of clinical investigation *99*, 2644-2654.

Srinivas, S., Watanabe, T., Lin, C.S., William, C.M., Tanabe, Y., Jessell, T.M., and Costantini, F. (2001). Cre reporter strains produced by targeted insertion of EYFP and ECFP into the ROSA26 locus. BMC developmental biology *1*, 4.

Stanley, E.G., Biben, C., Elefanty, A., Barnett, L., Koentgen, F., Robb, L., and Harvey, R.P. (2002). Efficient Cre-mediated deletion in cardiac progenitor cells conferred by a 3'UTR-ires-Cre allele of the homeobox gene Nkx2-5. The International journal of developmental biology *46*, 431-439.

Sturzu, A.C., Rajarajan, K., Passer, D., Plonowska, K., Riley, A., Tan, T.C., Sharma, A., Xu, A.F., Engels, M.C., Feistritzer, R.*, et al.* (2015). Fetal Mammalian Heart Generates a Robust Compensatory Response to Cell Loss. Circulation *132*, 109-121.

Takahashi, K., and Yamanaka, S. (2006). Induction of pluripotent stem cells from mouse embryonic and adult fibroblast cultures by defined factors. Cell *126*, 663-676.

Taniura, H., Taniguchi, N., Hara, M., and Yoshikawa, K. (1998). Necdin, a postmitotic neuron-specific growth suppressor, interacts with viral transforming proteins and cellular transcription factor E2F1. The Journal of biological chemistry *273*, 720-728.

Tatsumoto, T., Xie, X., Blumenthal, R., Okamoto, I., and Miki, T. (1999). Human ECT2 is an exchange factor for Rho GTPases, phosphorylated in G2/M phases, and involved in cytokinesis. The Journal of cell biology *147*, 921-928.

Tian, Y., Liu, Y., Wang, T., Zhou, N., Kong, J., Chen, L., Snitow, M., Morley, M., Li, D., Petrenko, N.*, et al.* (2015). A microRNA-Hippo pathway that promotes cardiomyocyte proliferation and cardiac regeneration in mice. Science translational medicine *7*, 279ra238.

Tucker, J.B. (1971). Microtubules and a contractile ring of microfilaments associated with a cleavage furrow. Journal of cell science *8*, 557-571.

Uosaki, H., Cahan, P., Lee, D.I., Wang, S., Miyamoto, M., Fernandez, L., Kass, D.A., and Kwon, C. (2015). Transcriptional Landscape of Cardiomyocyte Maturation. Cell reports *13*, 1705-1716.

Viatour, P., Somervaille, T.C., Venkatasubrahmanyam, S., Kogan, S., McLaughlin, M.E., Weissman, I.L., Butte, A.J., Passegue, E., and Sage, J. (2008). Hematopoietic stem cell quiescence is maintained by compound contributions of the retinoblastoma gene family. Cell stem cell *3*, 416-428.

von Gise, A., Lin, Z., Schlegelmilch, K., Honor, L.B., Pan, G.M., Buck, J.N., Ma, Q., Ishiwata, T., Zhou, B., Camargo, F.D.*, et al.* (2012). YAP1, the nuclear target of Hippo signaling, stimulates heart growth through cardiomyocyte proliferation but not hypertrophy. Proceedings of the National Academy of Sciences of the United States of America *109*, 2394-2399.

Warburg, O. (1925). The metabolism of carcinoma cells. J Cancer Res *9*, 148-163.

Xiao, G., Mao, S., Baumgarten, G., Serrano, J., Jordan, M.C., Roos, K.P., Fishbein, M.C., and MacLellan, W.R. (2001). Inducible Activation of c-Myc in Adult Myocardium In Vivo Provokes Cardiac Myocyte Hypertrophy and Reactivation of DNA Synthesis. Circulation research *89*, 1122-1129.

Xin, M., Kim, Y., Sutherland, L.B., Murakami, M., Qi, X., McAnally, J., Porrello, E.R., Mahmoud, A.I., Tan, W., Shelton, J.M.*, et al.* (2013). Hippo pathway effector Yap promotes cardiac regeneration. Proceedings of the National Academy of Sciences of the United States of America *110*, 13839-13844.

Xin, M., Kim, Y., Sutherland, L.B., Qi, X., McAnally, J., Schwartz, R.J., Richardson, J.A., Bassel-Duby, R., and Olson, E.N. (2011). Regulation of insulin-like growth factor signaling by Yap governs cardiomyocyte proliferation and embryonic heart size. Science signaling *4*, ra70.

Yang, X., Pabon, L., and Murry, C.E. (2014). Engineering adolescence: maturation of human pluripotent stem cell-derived cardiomyocytes. Circulation research *114*, 511-523.